Modeling and Performance Analysis of Direct Acting Valve Train System

Student: **Mr. Arslan Ahmad**

Regn.no. 2010-NUST-MS-I&ME-03

Supervisor

Dr. Riaz A. Mufti

School of Mechanical and Manufacturing Engineering (SMME)
National University of Science and Technology (NUST),
Sector H-12, Islamabad, Pakistan
(February 2013)

FORM TH-4

MASTER THESIS WORK

We hereby recommend that the dissertation prepared under our supervision by: (Student Name & Regn No.) Mr. Arslan Ahmad & 2010-NUST-MS-IME-03 Titled: Modeling and Performance Analysis of Direct Acting Valve Train System be accepted in partial fulfillment of the requirements for the award of MS degree with Grade ___.

Examination Committee Members

1. Name: Dr. Liaqat Ali Signature:_____

2. Name: Dr. Nabeel Anwar Signature:_____

3. Name: Dr. Samiur Rahman Signature:_____

Supervisor's name: Dr. Raiz A. Mufti Signature:_____

Date:_____

---------- ----------

Head of Department Date

Countersigned

---------- ----------

Dean/Principal Date

Dedicated To

My Parents

Certificate of Originality

The contents of this thesis are the original work of the author and reference has been mentioned, where required. Any portion of this thesis has not been previously accepted for any degree, and it is not being presently submitted in candidature of any degree.

Arslan Ahmad

(10-NUST-MS-IME-03)

Thesis Scholar

Countersigned

Dr. Riaz A. Mufti

Thesis Supervisor

Table of Contents

List of Figures

List of Variables

v = Velocity of tappet

L_f = Lift of tappet

t = Time

θ= Degree

e_1-e_2 = Eccentricities due to tappet tilting

m=Spring mass

M=mass of moving parts

k =spring stiffness

S= Spring force

V_c =Velocity of contact point with respect to cam

V_f = Velocity of contact point with respect to follower

V_e=Entraining velocity

V_s=Sliding velocity

p = Pressure distribution

p_{max}=Maximum hertzian stress pressure

b =Contact half width

W= Contact load

W_a = Asperity load

E'=Equivalent elastic modulus

R=Radius of curvature

r_b =Base circle radius

r_c =Cam radius of curvature

r_f =Follower radius of curvature

h_{min}= Minimum film thickness

h_{cen} = Central film thickness

G= Dimensionless speed parameter

U= Dimensionless speed parameter

W'=Dimensionless load parameter

η_0= Viscosity at atmospheric pressure and lubrication temperature

H=Power loss

F=Friction due to shear

μ_{lim} =Limiting coefficient of friction

°F=Fahrenheit

°C=Degree Celsius

c = clearance between follower guide interface

d =Valve diameter

ζ= Follower tilting

γ=Rate of change of shear stress with pressure

ε_1 = Dimensionless eccentricity of bottom half follower

ε_2 = Dimensionless eccentricity of bottom half follower

Ω=Tappet rotational speed

α =Pressure-Viscosity Coefficient

ω=Camshaft speed

τ_0 = Eyring stress of lubricant

τ_L =Limiting shear stress

π=Pi

σ_c=Roughness height of Cam

σ_f=Roughness height of follower

σ =Composite roughness height of cam/follower

η= Dynamic viscosity of lubricant within tappet/bore

A_a = Apparent area of contact

D_f=Diameter of follower

J= Moment of inertia of follower

F_c = Friction at cam/tappet due to shear and asperity contact

Acknowledgement

All thanks to Allah Almighty who is the most Courteous and Forgiving who gave me the audacity and motivation to complete this research work. I accept with admiration the inspiring supervision, constant support, important suggestions and kind supervision of **Dr. Riaz A. Mufti** and **Dr. Yousaf Habib.**

I also want to state my deep gratitude to my **family members** who saved no endeavor to create the appropriate environment for thought and meditation.

Arslan Ahmad

Abstract

Engine manufacturers all around the world are trying to find ways to reduce fuel consumption during the engine operation to improve overall efficiency. Major fuel losses occur due to thermal and mechanical losses. The focus of this research work is on mechanical losses in engine valve train. Different researchers have developed valve train friction models to analyze the tribological performance of engine valve train. Valve train frictional loss is mostly due to the interaction between cam and tappet. Friction models developed by Yang (1992) and Zhu (1988) have been used with changes to develop new mathematical model to analyze the effect of lubrication on the friction at cam/tappet, tappet/bore and valve/stem interface. In these model effects of tappet rotation is also examined on friction and power loss.

Matlab software has been used to develop software for valve train friction. Different parameters like camshaft speed, dynamic viscosity etc. have been changed in the parametric study to analyze effects on minimum film thickness, vertical loading, friction due to asperities, shear friction and power loss.

Chapter 1

INTRODUCTION

1.1 Introduction:

The automobile industry is rapidly changing. This change is due to pressures from several fronts like higher customer expectations, fuel economy, safety, international competition is increasing, social pressures like regulations for emissions. That's why auto mobile industry has significantly advanced in the last decade. The changes are in terms of items like electronic engine controls which are not directly related to tribology, but which can impact tribological components. Some changes directly affect tribological components like changes in engine design. [36]

For designing new engines researchers are not only trying to improve the performance but lowering the overall fuel consumption is also important. Different researchers have investigated the reasons for losses in internal combustion engine and methods to reduce them e.g. Parker and Adams (1981), Martin (1985). Their findings suggest that major losses are because of thermal inefficiencies, however there is still potential for the reduction of fuel consumption by lowering the mechanical losses. Approximately 15% of the total fuel consumption can be reduced by reducing mechanical losses [1]. 7.5% to 21% of the overall mechanical losses are due to the valve train friction [39].

In the past few years several mathematical models have been developed to evaluate the effect of friction on the overall efficiency of engine. In this study a new model of engine valve train is developed by making changes in the previously developed models namely Yang (1992) and Zhu (1988). In this model tappets rotation, tilting of tappet in the bore, friction due to asperities is considered. Matlab Model has been developed for this mathematical model.

Parametric study has been carried out using the program developed so as to analyze the changes in kinematic and tribological performance of direct acting cam. Factors like camshaft speed, dynamic viscosity of lubricant, limiting coefficient of friction has been changed to see the effects on minimum film thickness, shear friction and vertical loading.

Aim:

To Model, Simulate and Analyze the effects of minimum film thickness, friction, tappet rotation and surface roughness on engine valve train performance

Objectives:

1. To develop a Matlab Model for Valve Train Friction
2. Different parametric studies will be conducted to analyze engine performance at different cam shaft speeds, oil viscosity

Chapter 2
Literature Review

2.1 Valve Train Design:

Before the design of engine valve train, several parameters have usually been decided like engines displacement, desired performance of engine, the bore and stroke and the maximum cost of assembly and manufacturing. The valve train system choice is controlled by these parameters.

If the performance requirement is such that the valve must open and close rapidly, this indicates that around the cam flanks very high accelerations are required. So now push rod mechanisms would not be used as they are not flexible. This leaves the direct acting mechanism as the only option. Now the designer has to decide whether the tappets with large diameters needed for direct acting system can be fitted into the available space [31].

If the designers choose other type of valve train system then they must decide on the basis of advantages and disadvantages of that system and whether the system can fulfill the performance requirement.

After deciding the type of mechanism, the geometry of mechanism must be designed. The cams maximum eccentricity during the operation dictates the tappet diameter. This can be found directly from the velocity of the valve [9].Then the designer can estimate whether space between the valves can accommodate the tappets. After the estimation of tappet size, the equivalent mass of the valve train parts can be decided. To prevent the valve bounce, minimum spring stiffness is calculated on the basis of maximum speed of engine and valve acceleration. The dimensions of valve spring are decided on the basis of available space, number of working coils, fatigue life and wire diameter, complete details to these aspects are discussed by Beard and Hempson (1962).

In order to decide the size of cam, following factors are considered: engine height, cam bearing diameter, maximum hertzian stress, sliding speed and the lubrication conditions throughout the cam cycle.

2.2 Overhead Cam: Advantages and Disadvantages

Design of valve train has been subject to change for the last decades. The reason is that the engine manufacturers have experienced several problems like wearing of valve train [30]. That's why various valve train designs have been developed to reduce warranty claims and loss in sales. These designs include poppet valve and sleeve or rotary valves. Rotary valves consume oil excessively, frictional losses are high and the sealing is quite poor [2].

Due to the demand for increasing efficiency of engines, overhead cam mechanisms have been famous because of this reason. The overhead cam mechanisms use push rod systems. There are several advantages of push rod systems like good lubrication, due to the reason that the location of camshaft is near the oil sump so it receives lubricant in the form of splashes from crankshaft, low wear and adjustment is quite easy. The tappets in OHC are free to rotate, so the wearing of tappets is less as the entrainment of lubricant is high [31].

However there are disadvantages related to push rod mechanism, one of them is the usage of thin long pushrods. Due to this they are not fit for engines with high speeds. The popularity decline of push rods is also due to recent techniques used in production. There are fewer parts in OHC mechanisms which allow the production of cylinder assembly as a separate unit. Engineers recognize this as a great disadvantage [28].

There are two basic types of OHC systems, one is via a pivoted tappet and the other is direct acting. The alignment of camshaft and tappets is one of the problems during manufacturing of these types of OHC mechanisms. Due to this misalignment the contacting bodies suffer edge loading causing damage. Mercedes solved this problem by making end pivoted tappets which are located on spherical ended posts, so the tappets self aligns itself.

The direct acting OHC systems have been successful with regard to wear and performance .On the other hand the pivoted OHC systems have not performed well. Researchers suggested that this is caused by the adoption of electric fans that are thermostatically controlled and the usage of more selective channels for coolants throughout the engine, due to this there is an increase in temperature in the cylinder heads. This temperature rise increases the possibility of scuffing [9]. The tappets have limited ways to remove heat generated in the contact region, so this increases

the bulk temperature in the tappets. Other suggestions for the problems in such mechanisms have been fuel dilution of the lubricating oil and starvation of oil at engine startup [31].

These problems in pivoted OHC mechanisms can be solved by using spray bars and high specification materials. The cam lobes have holes to supply lubricant to the contact region. This helps to lubricate the contact and keep it cool.

OHC mechanisms have other drawbacks aside from poor wear properties. The oil and fuel pump and other auxiliaries are driven by the camshaft, so if these parts are to be driven by the camshaft, they should be mounted very high in the engine. While using OHC system it is important to drive the oil pump using crankshaft so that the distance between the pump and sump is small. This however increases the total engine length and may cause lubricant aeration. In the OHC system the flexing of the valve train mechanism occur in the camshaft. If the camshaft derives the distributor this may cause ignition timing issues [31].

2.3 Lubrication of Cam and tappet:

During the contact of cam and tappet different lubrication regimes are present which are explained below.

2.3.1 Modes of Lubrication:

2.3.1.1 Fluid Film Lubrication:

If the layer of the lubricant is so thick that the bodies cannot come into contact, such type is called ‘fluid film lubrication’. This type of lubrication is considered as ideal for reducing friction and wearing of bodies in contact. The contact behavior is mainly governed by the physical properties of the lubricant like viscosity, and due to the viscous shearing of the lubricant the characteristics of the friction arise [31].

2.3.1.2 Boundary Lubrication:

If the lubricant film thickness is so small that the surfaces of the bodies are in contact over an area that is similar to the area formed during the dry contact, such type of lubrication is called ‘boundary lubrication’. The friction characteristics are determined by both the solid and lubricant properties.

The lubricant film in this case is of molecular proportions. The chemical and physical properties of this thin film govern the contact characteristics. Bulk lubricant properties don’t affect the

characteristics and the friction coefficient doesn't depend on viscosity [30]. In case of cam and tappet, some element of boundary lubrication may be present around the nose of the tappet [1]

2.3.1.3 Elastrohydrodynamic Lubrication:

Elastrohydrodynamic lubrication is a form of fluid film lubrication. This type of lubricant regime occurs due to elastic deformation of the solid materials. It generates readily in highly stressed line or point contacts e.g. cam and tappet, gears and rolling bearings. This type of lubrication mostly occurs between non conformal contacts [1]. In non conformal contacts there is high pressure between the lubricated contact and surfaces are elastic [23] as shown in figure 2.1. In this type of regime the lubricants viscosity increases to large extents due to the large contact pressures. The viscosity of lubricant may increase to several thousand times in comparison to the lubricant viscosity at atmospheric temperature and pressure.

At the cam flanks if the cam shaft speed is high and contact is supplied with appropriate amount of lubricant than EHL may occur as the entrainment velocity is high at the flanks

2.3.1.4 Hard Elastrohydrodynamic Lubrication:

This occurs in solid materials which are non conformal and have large elastic modulus e.g. Cam and tappet, gear teeth, roller bearings etc. As the surfaces do not conform, the concentration of the load is on elastically deformed, small areas. Pressure of the lubricant oil film in these contacts ranges as high as .5 to 3 GPa, thousand times greater than in hydrodynamic contacts. [11]

2.3.1.5 Mixed Lubrication:

In the past, engineers only considered the full film lubrication and boundary lubrication, but different mechanisms operate in 'mixed lubrication' which is between these two regimes. As already mentioned above that in full fluid lubrication the bodies are completely separate, and in boundary lubrication the conditions are according to dry contact. Speed, Load and apparent area of contact doesn't affect friction coefficient. [31].

The characteristics of the contact in mixed lubrication are governed by both the boundary and full film lubrication. The chemical and physical properties of these regimes are important in mixed lubrication. Many components of machines operate in the 'fluid film', 'mixed' and 'boundary' regimes at different instances. With regard to cam and tappet

contact, mixed lubrication may be present at the interface if EHL contact is not present due to the unavailability of adequate lubricant at the contact [1].

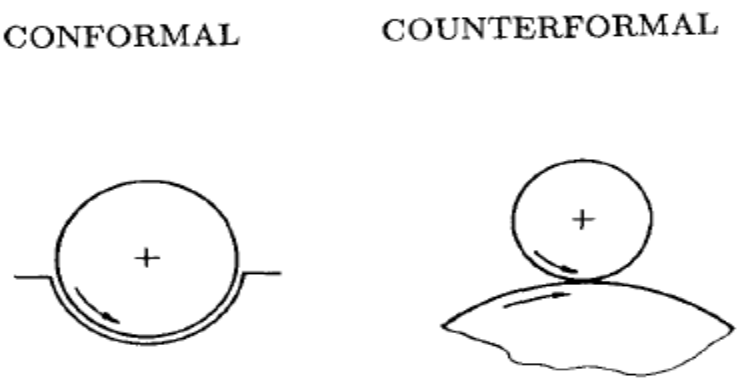

Figure 2.1 Conformal and Non Conformal contact [23]

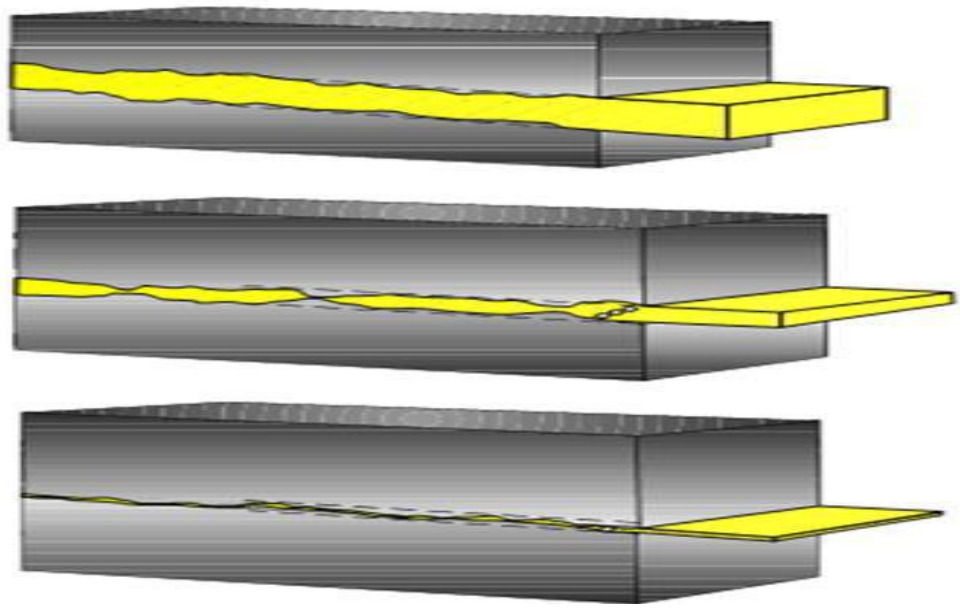

Figure 2.2 Different Lubrication Regimes (a) Full Film (b) Mixed (c) Boundary

The figure 2.3 shows variation of coefficient of friction with film thickness ratio. It shows that cam and follower operate in boundary, mixed, elastrohydrodynamic regimes. Figure 2.3 shows that hydrodynamic lubrication has film thickness ratio between 10 to 100.For elastrohydrodynamic lubrication the film thickness ratio is greater than 4 or 5.Mixed lubrication has thickness ratio between 1-5 and for boundary lubrication it is less than 1.

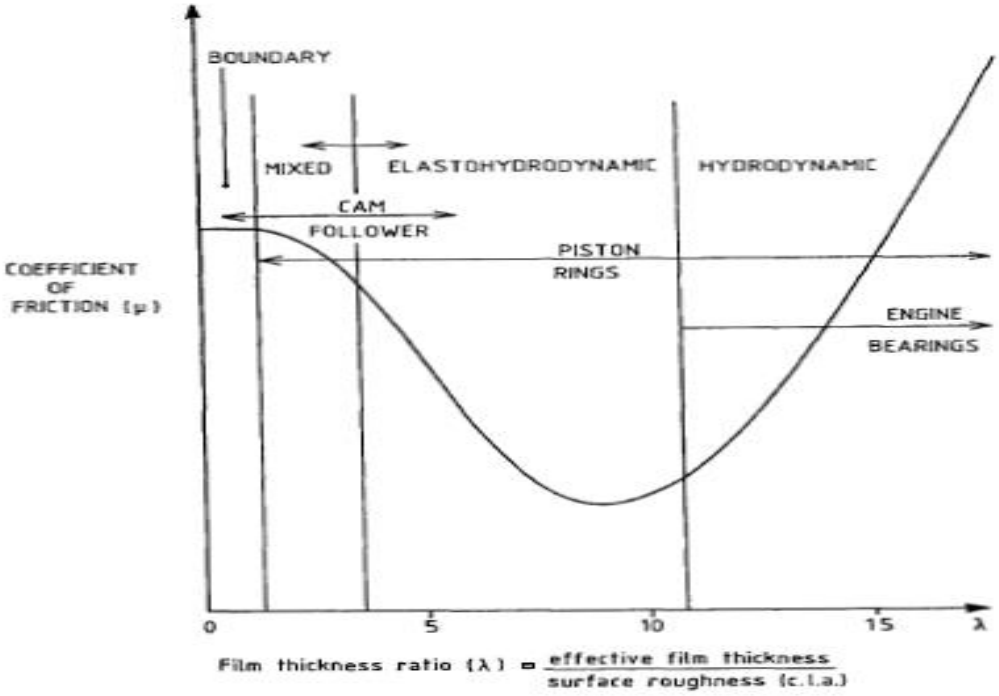

Figure 2.3 Coefficient of Friction variations with Film Thickness Ratio [31]

2.4 Rotation of Tappet:

Cam and tappet centers are eccentric so that the followers can rotate. Due to the rotation of tappet the researchers have seen a reduction of wear and friction loss in direct acting cam and follower. The working point of load is moving over the tappet face so that the tappet pivoted on the edge of the valve tilts. [15] Research has been done on the effect of follower rotation on oil film thickness and characteristics of friction. Pieprzak et al. (1989) and Willermet et al (1989) have worked on follower rotational motion. They conclude that the follower rotational speed increases as the camshaft speed increases and friction decreases. The reason they gave for this kind of effect was the partial rolling movement on the surface of contact rather than the increase in oil film thickness. Monteil et al. (1996) measured follower rotation through experimentation and concluded that the rotation of tappet is controlled by complex factor. Gecim (1992) measured tappet rotation and found that friction loss can be reduced by follower rotation.

Chapter 3

Mathematical Methodology

3.1 Kinematics of Cam and Follower:

Kinematic analysis of cam and follower is done by (Dyson and Naylor 1960).Here kinematics of direct acting cam and flat faced follower is discussed, as the engine under study has direct acting cam and flat faced follower.

The contact between a flat faced follower and a cam is shown in the figure 3.1 .Designation of cam is number 1 and tappet is number 2. In this study, tappet rotation about z axis is also considered, where as in yang's model the tappet rotation is not considered. The cam is rotating about its center O .Cam's instantaneous radius of curvature is designated by O'. The tappet only moves in the z direction so its velocity in the x direction is zero. The velocity of tappet in the z axis can be calculated by the given equation 3.1

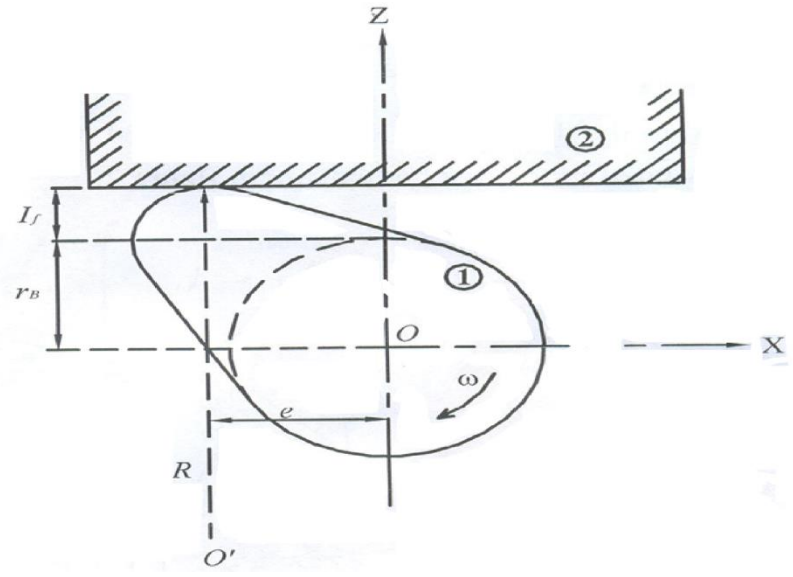

Figure 3.1 Direct acting cam and tappet [30]

$$v = \frac{dL_f}{dt} = e\omega \qquad (3.1)$$

The eccentricity of the cam can be calculated by the equation given below

e =v/ω (3.2)

The acceleration of tappet can be can be calculated by the given formula given below

a = $\frac{d^2L_f}{d^2t} = \omega\frac{de}{dt}$ (3.3)

The cam velocity at the contact point is u_1 which is expressed as:

$u_1 = (r_b + L_f)\omega$ (3.4)

In the x direction with respect to the cam, the contact point velocity is given by

$V_C = u_1 - u$ (3.5)

Here u is the contacts velocity which can be expressed as -$\frac{de}{dt}$, the negative sign shows a decrease in eccentricity as the contact point moves in the x axis.

Tappet's velocity at the contact point is u_2, which is zero. In the x direction with respect to tappet the contact point velocity is

$V_f = u_2 - u$ (3.6)

Substituting Equation 3.3 into Equation 3.6

$V_f = \frac{de}{dt} = a/\omega = \omega\frac{d^2L_f}{d\cdot\theta^2}$ (3.7)

Equation 3.5 can be written as

$V_C = (r_b + L_f)\omega + \frac{de}{dt}$ (3.8)

or

$V_C = \left[(r_b + L_f) + \frac{de}{d\theta}\right]\omega$ (3.9)

As

$$\frac{de}{dt} = \frac{de}{d\theta}\frac{d\theta}{dt} = \frac{de}{d\theta}\omega \qquad (3.10)$$

From equation 3.7 and 3.10

$$\frac{de}{d\theta} = \frac{d^2L_f}{d\cdot\theta^2} \qquad (3.11)$$

At last equation 3.9 becomes

$$V_C = \left[\left(r_b + L_f\right) + \frac{d^2L_f}{d\cdot\theta^2}\right]\omega \qquad (3.12)$$

3.2 Radius of Curvature:

The instantaneous radius of curvature for flat faced follower is expressed as,

$$R = V_C / \omega \qquad (3.13)$$

Putting equation 3.12 into equation 3.13

$$R = \frac{d^2L_f}{d\cdot\theta^2} + L_f + r_b \qquad (3.14)$$

3.3 Sliding velocity:

Sliding velocity between cam and follower is given as

$$V_s = V_C - V_f \qquad (3.15)$$

Putting equation 3.7 and 3.12 into equation 3.15, V_s becomes

$$V_s = \left[\left(r_b + L_f\right) + \frac{d^2L_f}{d\cdot\theta^2}\right]\omega - \omega\frac{d^2L_f}{d\cdot\theta^2} \qquad (3.16)$$

3.4 Mean entraining velocity

Entraining velocity can be found by taking the mean of the velocity of both the surfaces and is given below

$$V_e = \frac{1}{2}(V_C + V_f) \qquad (3.17)$$

Putting equation 3.7 and 3.12 into equation 3.17,V_e becomes

$$V_e = \frac{1}{2}\left\{\left[\left(r_b + L_f\right) + \frac{d^2 L_f}{d\cdot\theta^2}\right]\omega + \omega\frac{d^2 L_f}{d\cdot\theta^2}\right\} \qquad (3.18)$$

3.4 Calculation of Contact Loading:

In this part, we are going to calculate the loading on cam and follower interface. It is difficult to accurately calculate the load that can be carried by the contact between cam and follower. The forces that are generally associated with this operation are listed below:

- Inertia force
- Spring force
- Forces due to stiffness and damping characteristics of different components
- Friction forces resulting from the contact between components

In this study damping and deflection forces are omitted by assuming that the valve train is rigid. This assumption makes it easy to calculate contact loading due to spring and inertia forces. Inertia force is calculated by summing the mass of moving parts and multiplying it by the acceleration of moving parts [30].

$$I = \left(M + \frac{1}{3}m\right)a \qquad (3.19)$$

Spring force S is equal to the deflection of the spring multiplied with the spring stiffness.

$S = k(I_f + \delta)$ (3.20)

Total load acting cam/follower interface, here weight and friction components are neglected.

$W = S + I$ (3.21)

Putting equations 3.19, 3.20 into equation 3.21

W= (M+1/3 m)*a + k*(I_f+δ) (3.22)

Hydraulic lash adjuster keeps the cam and follower in contact with each other. Load over the cam base circle is dependent on

- Lash adjuster fluid pressure
- Compression force of check valve spring
- Plunger area

The load over the cam base circle is determined by multiplying cam inlet lubricant pressure with plunger area. It is assumed that the valve spring force is very small, so it is neglected [30]. So the equation 3.22 becomes

$W = \left(M + \frac{1}{3}m\right)a + k(I_f + \delta) + \mathrm{P} \times \mathrm{A}$ (3.23)

3.5 Calculation of Contact Pressure:

After the determination of contact loading at the interface of cam and follower, the prediction of maximum hertzian contact pressure and the dimension of the area of contact can be done, using Hertz contact theory of elastic contact (Hertz 1882).

The contact between a cam and a tappet is geometrically similar to that of a cylinder against a plane. According to Hertz theory line contact is formed between cam and flat tappet as shown in the figure 3.2 .It also shows the hertzian contact patch formed by the line contact.

The assumptions of the Hertzian contact theory of elastic contact are stated below:

1. Bodies in contact are elastic and fulfill the criterion of Hooke's Law.

2. The area of contact between the bodies is smaller, compared to the radius of curvature of a cylinder that is undeformed.
3. Normal pressures are taken into consideration only.

Figure 3.3 shows that for a line contact between bodies, the pressure distribution is semi elliptical, and is expressed as

$$p = p_{max}(1 - \frac{x^2}{b^2})^{1/2} \quad (3.24)$$

In the equation 3.24, b is the contact half width

$$b = (8WR/\pi LE')^{1/2} \quad (3.25)$$

R is the equivalent radius of curvature, which is expressed as

$$\frac{1}{R} = \frac{1}{r_c} + \frac{1}{r_f} \quad (3.26)$$

The term $\frac{1}{r_f}$ is zero as the radius of curvature of the flat faced tappet is infinite. At the center of the rectangular boundary P_{max} acts and is given by

$$P_{max} = \frac{2W}{\pi L b} \quad (3.27)$$

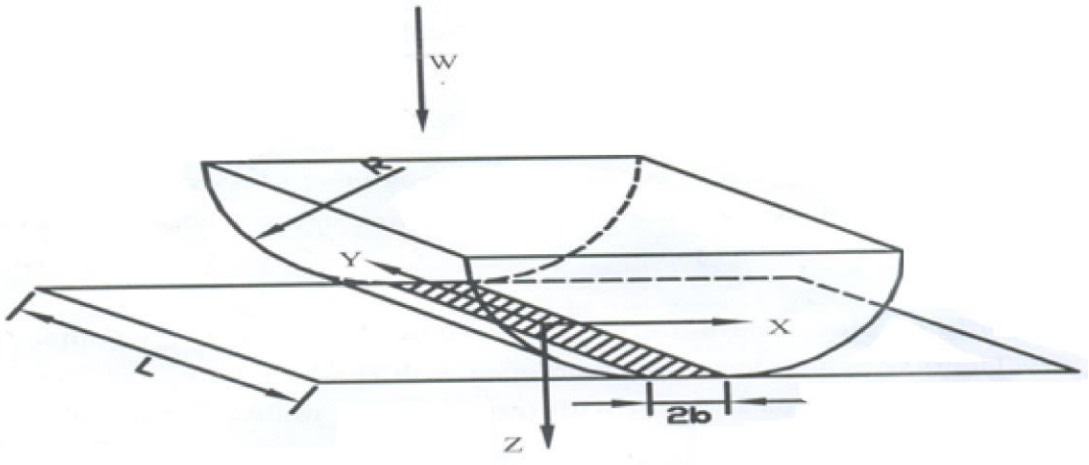

Figure 3.2 Contact between Plane and Cylinder-Hertzian Contact Patch [31]

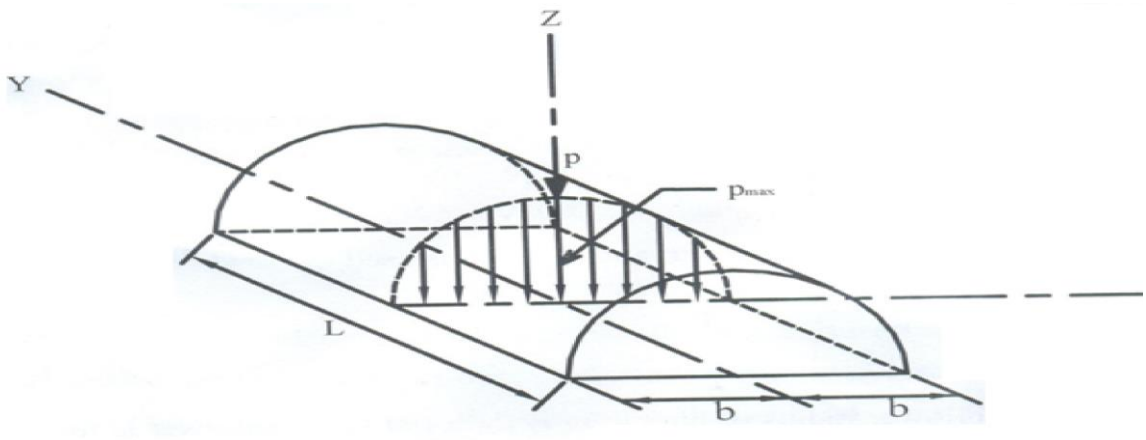

Figure 3.3 Pressure distribution of line contact [31]

3.6 Calculation of Lubrication Film Thickness:

Three types of Lubrication regimes are found during the contact between cam and tappet. These regimes are boundary, hydrodynamic and elastrohydrodynamic lubrication. If classical theory of hydrodynamic lubrication is applied at the contact of cam and tappet, very small film thickness is found. As these heavily loaded components have long operational life, boundary and hydrodynamic lubrication doesn't protect the surfaces at such high loads. Here elastrohydrodynamic lubrication plays its part. EHL forms between non conformal components, when very high pressures are generated. This pressure can be of the order of hundreds of mega Pascal or even Giga Pascal. As the pressure is so high that the viscosity of lubricant increases and lubricant shows nearly solid like characteristics (30).

If the supply of oil reaches the contact adequately, full separation between the contacting bodies is not guaranteed. Different formulae are available for measuring the minimum and central film thickness.

To find minimum film thickness between two smooth cylinders in a line contact (Dowson and Higginson 1977) developed a formula, which is given as

$$\frac{h_{min}}{R} = 2.65\, U^{.70}\, G^{.54}\, W'^{-.13} \qquad (3.28)$$

Dowson and Toyoda (1979) developed a similar formula for measuring the central film thickness.

$$\frac{h_{cen}}{R} = 3.06\, U^{.69}\, G^{.56}\, W'^{-.10} \qquad (3.29)$$

Squeeze film is also present around the parts of cam cycle where the lubricant entrainment is less, so the accurate measurement of film thickness through above formulae is difficult under such conditions. But for quasi steady state analysis which is used to qualitatively analyze the engine valve train design, these formulae can be used. (30)

The parts of components where surface contact occurs over an area which is similar to the area formed in dry contact, Boundary lubrication is present in those parts. Boundary lubrication may be present around the cam nose where the entrainment velocity is medium and loads are high. Law of dry friction is generally used during such conditions because the friction coefficient doesn't depend on the viscosity, load, contact area and speed (30).

3.7 Baraus Law:

The lubricant viscosity changes with changing pressure. The Baraus equation describes the relationship between pressure and viscosity. It is given below

$$\eta = \eta_o \,.\, e^{\alpha p} \qquad (3.30)$$

As shown by the equation 3.30, η varies exponentially with pressure; the viscosity will be extremely high when pressure is high.

Chapter 4

Asperity Interactions

4.1 Asperity Interactions:

Experimental and theoretical research has proved that the surface roughness influences the tribological characteristics of the tappet and cam [38]. Surface roughness impact on the tribological characteristics wasn't included in the yangs model. But in this study asperity interactions have been included. The model being used to study asperity interactions was developed by (Greenwood and Tripp 1970). Through this model real area of contact and asperity contact force can be found.

4.2 Calculation of Asperity Contact Load:

This model is based on the assumption of a Gaussian distribution of asperity heights and contact radius of curvature of the symmetric asperities. Elastic asperity deformation is taken into account in this study.

$$W_a = \frac{8\sqrt{2}}{15}\pi(\beta\sigma\eta)^2 E' \left(\frac{h}{\sigma}\right) A\, F_{\frac{5}{2}}\sqrt{\frac{\sigma}{\beta}} \qquad (4.1)$$

Where σ is the composite roughness height and can be found by the equation given below

$$\sigma = \sqrt{\sigma_c^2 + \sigma_f^2} \qquad (4.2)$$

4.3 Calculation of the Real Area of Contact:

Actual and apparent area of contact are related through the equation 4.3, given below

$$A_a = \pi^2(\eta\beta\sigma)A\, F_2\left(\frac{h}{\sigma}\right) \qquad (4.3)$$

4.4 Calculation of asperity contact function:

Asperity contact functions can be found using the integrations given below:

$$F_2\left(\frac{h}{\sigma}\right) = \int_{\frac{h}{\sigma}}^{\infty}\left(s - \frac{h}{\sigma}\right)^2 e^{s^2/2} \qquad (4.4)$$

$$F_{\frac{5}{2}}\left(\frac{h}{\sigma}\right) = \int_{\frac{h}{\sigma}}^{\infty} \left(s - \frac{h}{\sigma}\right)^{\frac{5}{2}} e^{\frac{s^2}{2}} \qquad (4.5)$$

Chapter 5

Calculation of Friction and Total Power Loss

5.1 Introduction:

The overall friction associated with valve train assembly can be divided into four categories, which are listed below;

1) Friction arising from cam/tappet interface

2) Friction arising from follower/bush interface

3) Friction arising from valve stem/guide interface

4) Friction arising from valve stem/seal interface

These four categories are responsible for the valve train power loss. Valve stem /seal will not be included in this model; rest of them will be modeled in the following sections.

5.2 Calculation of Friction at Cam/tappet interface

5.2.1 Friction at the cam/tappet

Friction at the cam and tappet interface can be divided into two parts;

1) Friction caused by the shearing of the lubricant

2) Friction caused by the asperity contact

5.2.2 Friction due to shear force of between Cam/tappet

For the purpose of calculating friction, two assumptions are made which are given below:

- Elastrohydrodynamic lubrication is assumed between the cam and follower contact.
- At any moment the interface is isothermal

  Dry Hertzian contact can be used to predict the contact pressure and dimension because of the reason that the elastic deformation between cam and tappet is high in comparison with film thickness of the lubricant. As at the solid boundary, viscous friction force is proportional to the velocity gradient, by approximating the lubricant contact region at the cam/tappet interface as an area of constant film thickness(h_{cen}), using classical

elastrohydrodynamic theory, not taking into account rolling friction, prediction of sliding friction force can be done (30). Substituting the Baraus equation (3.30), we get the friction force

$$F_c^s = \int_{-b}^{b} \frac{\eta_o V_s \, e^{\alpha p}}{h_{cen}} \, dx \qquad (5.2)$$

Putting equation (3.24) in equation (5.2), the equation becomes;

$$F_c^s = \frac{\eta_o V_s \, e^{\alpha p_{max}}}{h_{cen}} \int_{-b}^{b} e^{\left(\frac{1-x^2}{b^2}\right)^{\frac{1}{2}}} dx \qquad (5.3)$$

As mentioned earlier the Baraus relationship shows that viscosity changes exponentially with pressure. So at large pressure, the viscosity will be extremely high, which predicts every large friction force [30]. To cater for this problem, in heavily loaded conformal contacts, limiting coefficient has been used. This limiting coefficient is dependent on the type and presence of friction modifier in the lubricant. The maximum limiting coefficient is found by testing under dry condition. So the friction at the cam/tappet interface can't go above the limiting coefficient. This model compares all the value of friction with limiting value at each degree of cam cycle, it utilizes the limiting value of friction if any friction value exceeds limiting value and assumes boundary lubrication.

$$F = \mu_{lim}.W \qquad (5.4)$$

5.2.3 Power loss at the cam/tappet interface:

At each degree of cam cycle power loss can be found by multiplying friction torque with angular speed of cam. Average power loss is calculated by taking integral of the cam cycle. Total power loss of the whole cam cycle will be modeled later. The equation can be given by;

$$H = \frac{1}{2\pi} \int_0^{2\pi} F_c^s \, . r . \omega . d\theta \qquad (5.5)$$

5.3 Friction Caused by the asperity contact:

Friction produced by the asperity contact of cam/tappet is assumed to be caused by the asperity sliding under the condition that boundary lubrication is present [23].

The friction force F_c^a can be calculated by the following formula

$$F_c^a = \mu_a W_a \qquad (5.6)$$

The formula used to predict the total friction at the cam/tappet interface takes into account the area of asperity contact. The formula is given below;

$$F_c = F_c^a + F_c^s(1 - \frac{A_a}{A}) \qquad (5.7)$$

5.4 Calculation of Friction at the tappet/bush interface

During Cam/tappet operation tappet tilts as it moves in the bore [38].This study is supported by the experimental research conducted in the past. As a result, a theoretical model [38] was developed to find friction between tappet/bore interface considering that tappet tilts during operation under conditions of boundary lubrication.

The model developed in this study is based on short bearing theory [29]. As it is very difficult to do full lubrication analysis of the tappet and bore, it requires complex numerical iterations and analysis and so it requires a lot of computing timing.

5.5 Tappet/bore Friction Model:

It is clear from figure 5.1, that tappet is tilting while it is in contact with the cam. The reaction forces that are caused due to this tilting W_{b1} and W_{b2} can be found by the given formula:

$$W_{b1} = W_{b2} - F_c \qquad (5.8)$$

$$W_{b2} = \frac{d}{L_f} W \qquad (5.9)$$

The movement of tappet in the bore is similar to that of a bearing with a shaft moving in a bush. As shown in the figure 5.1, the tappet shifts to the right-hand side so that it can balance the reaction force W_{b2} , causing the tappet to move a distance e_2 (eccentricity) .As the tappet is tilting in the bore this eccentricity is situated in the center of the tappets top half. Similarly balancing W_{b1} causes eccentricity e_1 which is situated in the center of tappets bottom half.

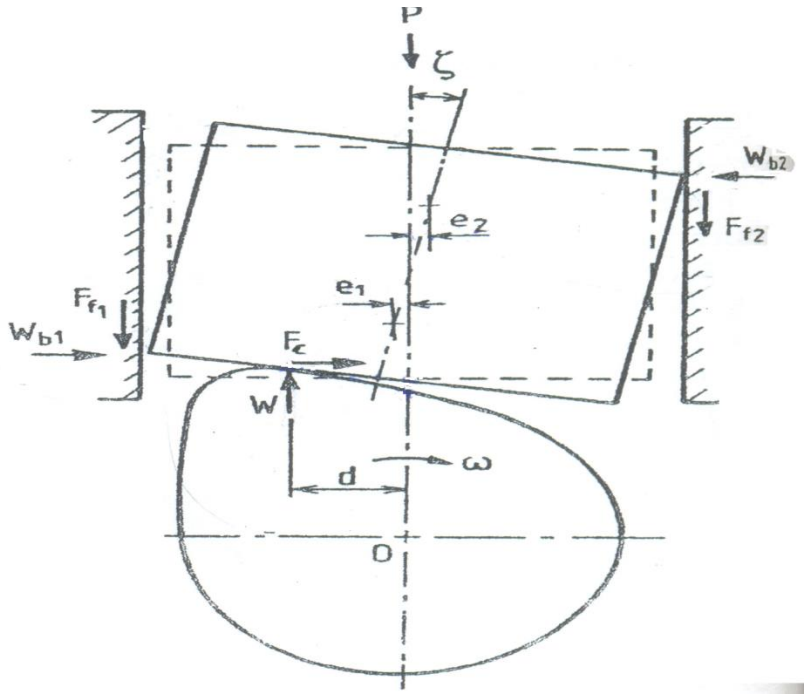

Figure 5.1 Tilting of Tappet in the Bore [39]

$$W_{b1} = \frac{\eta_b U L_f^3}{4C_f^2} \frac{\varepsilon_1}{(1-\varepsilon_1^2)^2} \sqrt{\pi^2(1-\varepsilon_1^2)^2 + 16\varepsilon_1^2} \qquad (5.10)$$

$$W_{b2} = \frac{\eta_b U L_f^3}{4C_f^2} \frac{\varepsilon_2}{(1-\varepsilon_2^2)^2} \sqrt{\pi^2(1-\varepsilon_2^2)^2 + 16\varepsilon_2^2} \qquad (5.11)$$

Where

$$U = \sqrt{v^2 + (\Omega D_f/2)^2} \qquad (5.12)$$

$$C_f = (D_b - D_f)/2 \qquad (5.13)$$

$$\zeta = arctan\left[\frac{2(e_1+e_2)}{L_f}\right] \qquad (5.14)$$

5.5.1 The Friction Modeling

As shown in the figure 5.1, due to the tilting of the follower near the top right and bottom left corner are critical contact location. That's why for the calculation of friction at these locations, minimum separations $C_{b1}$and C_{b2} is required [39]. The equation is given below:

$$C_{b1} = C_f - e_1 - \frac{L_f}{4}\tan(\zeta) \qquad (5.15)$$

$$C_{b2} = C_f - e_2 - \frac{L_f}{4}\tan(\zeta) \qquad (5.16)$$

Friction generated from the top half F_{f1} and the bottom half F_{f2} are calculated separately [39]. The total friction arising can be found by following equation.

$$F_f = F_{f1} + F_{f2} \qquad (5.17)$$

To determine the lubrication regime for the top and bottom half, the following formula can be used.

$$\lambda_{bfi} = \frac{C_{bi}}{\sigma_{bf}} \qquad (5.18)$$

If λ_{bfi} is less than 0, boundary lubrication is present at the contact interface [39]. The formulae for the calculation of friction in this condition are given as

$$F_{f1} = \mu_b W_{b1} \frac{\mathrm{v}}{U} \qquad (5.19)$$

$$F_{f2} = \mu_b W_{b2} \frac{\mathrm{v}}{U} \qquad (5.20)$$

If the value of λ_{bfi} is greater than 0 but less than 3, mixed lubrication regime is present at the follower/bore interface [39]. If there is mixed lubrication at the contact, friction has two parts:

1) Due to the contact of bodies.

2) Shear of the Lubrication

To determine the contribution of each part in the total friction, the following equation can be used:

$$\kappa_i = \frac{\lambda_{bfi}}{3} \qquad (5.21)$$

The total friction is given as:

$$F_{f1} = \left[(1-\kappa_1)\mu_b W_{b1} + \frac{\kappa_1 \pi U \eta_b D_f L_f}{2C_f\sqrt{1-\varepsilon_1^2}} \right] \frac{\mathrm{v}}{U} \qquad (5.22)$$

$$F_{f2} = \left[(1-\kappa_2)\mu_b W_{b2} + \frac{\kappa_2 \pi U \eta_b D_f L_f}{2C_f\sqrt{1-\varepsilon_2^2}} \right] \frac{\mathrm{v}}{U} \qquad (5.23)$$

If the value λ_{bfi} is greater than 3.0 than hydrodynamic lubrication regime is present at the interface [39]. The friction due to each half can be calculated by following formulae

$$F_{f1} = \left(\frac{\pi U \eta_b D_f L_f}{2C_f\sqrt{1-\varepsilon_1^2}} \right) \frac{\mathrm{v}}{U} \qquad (5.24)$$

$$F_{f2} = \left(\frac{\pi U \eta_b D_f L_f}{2C_f\sqrt{1-\varepsilon_2^2}} \right) \frac{\mathrm{v}}{U} \qquad (5.25)$$

Summarizing the friction formulae at the tappet and bore interface we get

$$F_{fi} = \mu_b W_{bi} \frac{\mathrm{v}}{U} \qquad \text{If} \quad \lambda_{bfi} < 0 \qquad (5.26)$$

$$F_{fi} = \left[(1-\kappa_i)\mu_b W_{bi} + \frac{\kappa_i \pi U \eta_b D_f L_f}{2C_f\sqrt{1-\varepsilon_i^2}} \right] \frac{\mathrm{v}}{U} \qquad \text{If} \quad 0 \le \lambda_{bfi} < 3 \qquad (5.27)$$

$$F_{fi} = \left(\frac{\pi U \eta_b D_f L_f}{2C_f \sqrt{1-\varepsilon_i^2}} \right) \frac{\mathrm{v}}{U} \quad \text{If} \quad \lambda_{bfi} > 3 \qquad (5.28)$$

5.6 Power Loss Model

By taking the product of the friction torque and the frequency of the camshaft, power loss can be calculated. Friction torque of the complete valve train can be divided into two parts.

1) Friction torque T_f due to sum of the friction of reciprocating parts and the eccentricity. Due to these frictions extra torque is needed to operate the camshaft. Formulation of reciprocating frictions like F_f and F_v has already been done. The total torque can be found by the formula stated below:

$$T_f = \left(F_f + F_v\right) * e \qquad (5.29)$$

2) Friction torque T_c due to the rotational friction of parts like the interaction between cam and follower. This friction torque can be calculated by the formula given below

$$T_c = F_c * e \qquad (5.30)$$

The total friction torque at each degree of cam angle θ can be expressed as

$$T_{fric} = T_f + T_c \qquad (5.31)$$

The power loss at each instant is calculated by taking a product of total friction torque T_{fric} and the rotational frequency of the camshaft. To find the overall powerless, integration over the whole cam cycle can be done. The equation is given below

$$\mathrm{H} = \frac{1}{2\pi} \int_0^{2\pi} \omega T_{fric} \, d\phi \qquad (5.32)$$

Chapter 6

Rotation of the Tappet

6.1 Calculation of Rotation of the Tappet:

Scuffing failure is serious types of damage which can be reduced by the rotation of tappet. This is done by designing the cam tappet in such a way that cam /tappet are not inline but at a certain offset. Extra component of velocity changes the direction and magnitude of the entrainment of lubrication due to the rotation of the tappet. As a result the condition of lubrication changes due to the rotation. To find out the frequency of rotation of the tappet is very important throughout the cam cycle. This chapter encompasses the mathematical model to find tappet rotation.

6.2 Modeling Rotation of the Tappet:

Cam/tappet is operational by using traction transmission principle. Friction at the interface of cam/tappet causes rotation of the follower. Friction due to the valve stem and plunger interface and follower/bush resists the tappet rotation. The system balance also affected when the tappet accelerates or decelerates [39]. Taking account of the all the above, the equation of the tappet rotation is developed from the torque balancing as shown in the figure 6.1 .The equation is given as:

$$J\dot{\Omega} = T_{fc} - T_{fb} - T_{fp} \qquad (6.1)$$

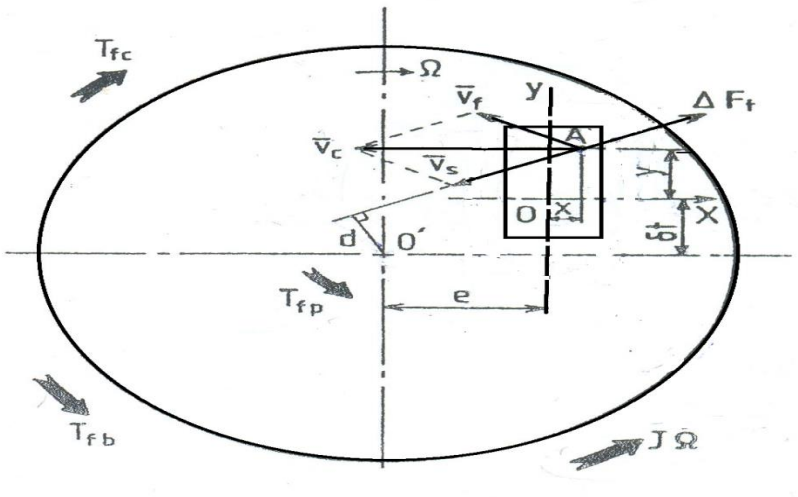

Figure 6.1 Moments acting on the tappet and in the hertzian contact [38]

6.3 Calculation of Driving Torque:

In the previous chapters overall friction model for cam/tappet was developed. The driving torque is due to the asperity contact at the interface of cam/tappet and the friction resulted from the lubrication shearing.

Figure 6.1 shows contact rectangular which is the Hertzian contact patch formed due to the interaction between cam and tappet. The origin of the coordinate system (xoy) is at the center of contact rectangle. The center of the contact rectangle is denoted O; contact center is at an offset e (eccentricity). Sliding velocity V_s keeps on changing as the tappet is rotating, so the driving torque also changes. Only a small portion of the contact patch causes rotation.

$$T_{fc} = d * F_c \qquad (6.2)$$

The friction due to tappet bore interaction is found by equation 6.3. Multiplying tappet/bore friction with tappet radius gives torque T_{fb} .

$$F_{fb} = \frac{\Omega D_f (F_{f1} - F_{f2})}{2\,\mathrm{v}} \qquad (6.3)$$

$$T_{fb} = \frac{\Omega D_f^2 (F_{f1} - F_{f2})}{4\,\mathrm{v}} \qquad (6.4)$$

Euler method can be used to find tappet rotation using iterative process. The reason for using this method is that T_{fb} is an implicit equation.

$$\Omega_{i+1} = \Omega_i + \dot{\Omega}_i (t_{i+1} - t_i) \qquad (6.5)$$

Chapter 7

Software Modeling and Solution Methodology

7.1 Computer Program:

A computer program has been developed in Matlab software, by using the friction model of valve train. Kinematic and tribological analysis has been done in this computer model. The analysis has been done for the performance of flat faced tappet. It mainly deals with the friction in cam/tappet, tappet/bore, valve stem /guide interface. Figure 7.1 is the flow chart for computer program of the valve train friction model, the main parts are:

- The tappet and Cam Kinematic analysis
- Tribological analysis of Cam and tappet
- Friction modeling of Valve and guide
- Friction modeling of tappet and bore
- Parametric study of valve train design

Matlab program picks the input values from a separate data file. All the input and output data is in SI units. Input data including the valve lift is from Ricardo Hydra Engine. As experimental data for valve lift is used so there is noise in the data.

As experimental valve lift values are used, the velocity and acceleration of tappet is found using numerical techniques. Cam angle is in degrees, which is converted to time. To calculate velocity the 2 point difference formula was used, for differentiating valve lift points with respect to time. Acceleration of the follower was calculated using 5 point difference formula, for differentiating Lift data with respect to time. Radius of Curvature, velocity of the contact point with reference to tappet and with respect to cam was calculated to find the entraining velocity of the cam/tappet interface.

In order to calculate the vertical loading at cam tappet interface, the program calculates inertia force due to the moving parts and spring force. It uses the hertzian contact theory to find the width of contact, equivalent radius of curvature and distribution of contact pressure.

The program calculates dimensionless material parameter, dimensionless speed parameter and dimensionless load parameter, to find the Minimum and central film thickness. Friction due to shearing of the cam/tappet surfaces is calculated by using the Simpson Quadrature Method. It integrates the shear friction for the whole hertzian contact at the cam/tappet interface.

In order to find the loading due to asperity contact the program calculates the actual area of contact. The eccentricities due to the tilting of tappet in the bore are calculated .These eccentricities are used to find the friction forces and supporting forces due to tappet and bore contact.

Balancing of torques due to tappet/bore friction, cam/tappet friction is used to find the rotational frequency of the tappet. The rotation of the tappet is found using a loop in which the value of tappet rotation converges. At each degree of cam angle the current and previous rotational frequency is compared to check for convergence. Flow chart for the measurement of Tappet rotation is shown in figure 7.2

The software calculates the power loss at each degree and then integrates to find the average power loss for the whole cam cycle. If the user wants to do a parametric study the software gives an option. Different design parameters can be changed to evaluate the overall performance of the valve train. Parameters that can be changed are cam shaft speed, dynamic viscosity of lubricant, limiting coefficient of friction, Radius of curvature, base circle radius of cam etc.

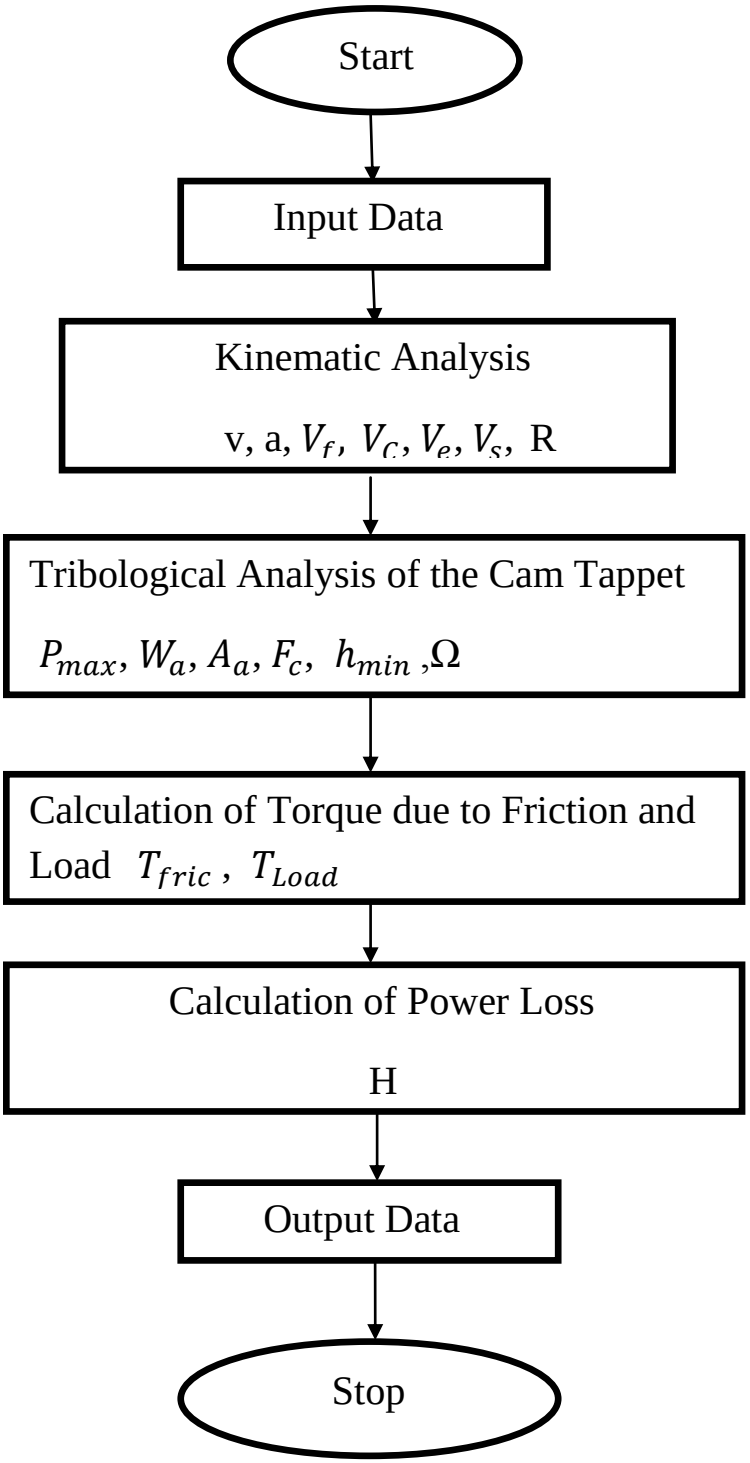

Figure 7.1 Direct Acting Valve Train Friction Model - Flow chart

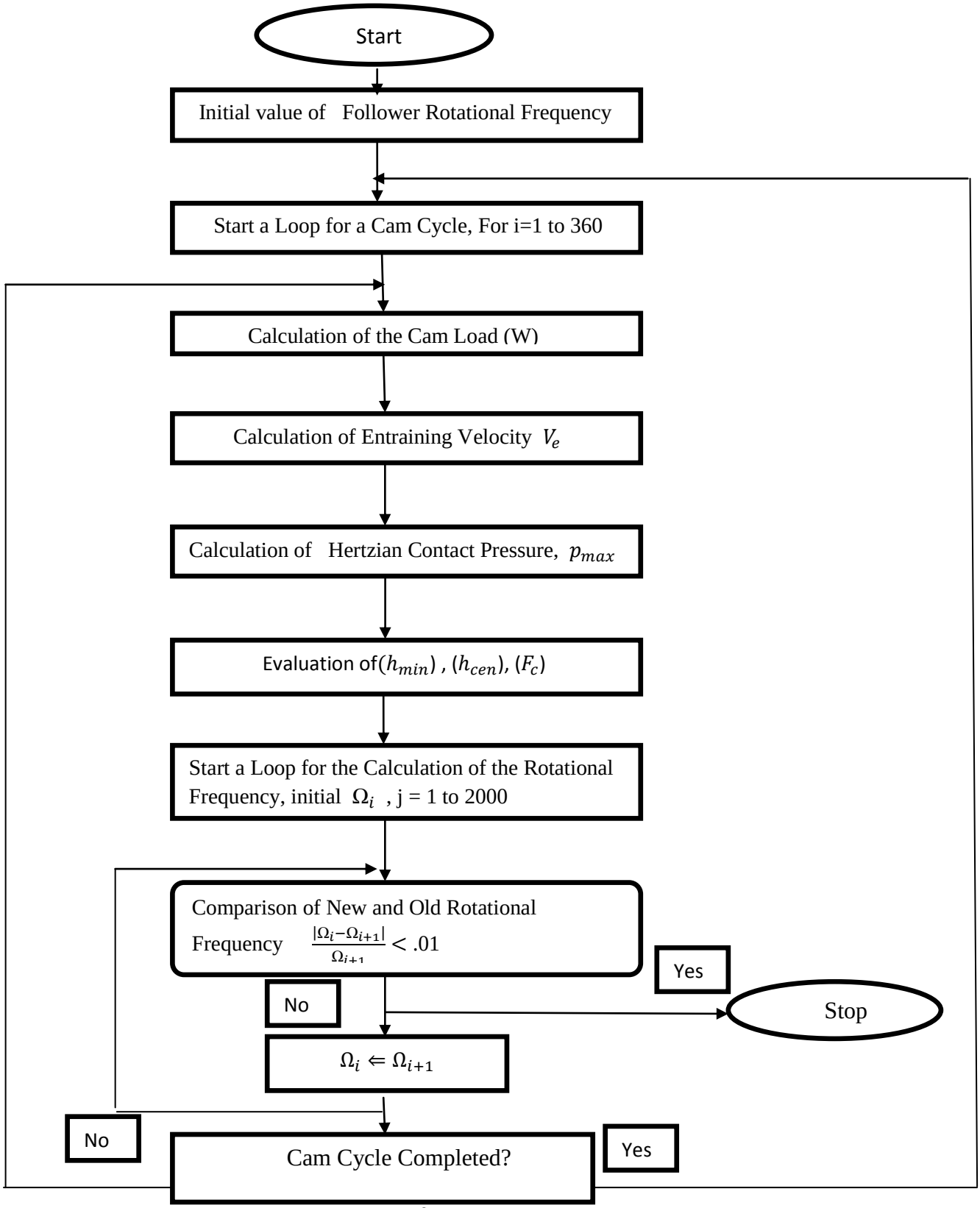

Figure 7.2 Measurement of Tappet Rotation-Flow chart

Chapter 8

Parametric Study

The program developed for cam and flat faced tappet is used to carry out a parametric study. Different parameters are changed like engine speed, lubricant temperature and limiting coefficient of friction to analyze the changes in engine performance. Parametric study can help to determine the design changes in the valve train, the type of friction modifier in lubricant, the minimum film thickness required to decrease friction at the cam/tappet contact, the affects of surface roughness and wearing of tappet on overall fuel consumption.

8.1 Affects of temperature variation from 40˚C to 95˚C at 400 RPM

First, the affects of changing lubricant viscosity will be analyzed at different camshaft speeds. The results indicate that at 400 rpm as the temperature of lubricant increases from 40˚C to 95˚C, the minimum film thickness decreases as shown in figure 8.4.The reason for this kind of behavior is that when the temperature increases the viscosity of lubricant decreases and the thickness decreases. At 40 C, the minimum thickness is greater at the flanks indicating that hydrodynamic film, so at the flanks the shear friction will be less as shown in figure 8.6 and as tappet rotation depends on torque produced by this friction so tappet rotation will be low too as shown in figure 8.7 .At the nose the thickness is .3 μm indicating that it is operating in boundary lubrication. At the nose of cam due to such film thickness the friction is high and also the tappet rotation is high, as shown in figure 8.6 and 8.7.As the lubricant viscosity decreases with increasing temperatures the minimum film thickness also decreases. At the flanks the thickness is 1.2 μm indicating the presence of elastrohydrodynamic lubrication and at the nose the thickness is merely .15 μm showing boundary lubrication. With the decrease in film thickness at the flanks and at the nose friction increases, the increase in friction is very small as shown in figure 8.6 due to the reason that as the shearing friction is greater than limiting value of friction the limiting value replaces the actual value. The tappet rotation also increase but the increase in value is small as shown in figure 8.7, the reason is that the increase in friction is small. During the increase in temperature, the vertical loading doesn't change as shown in figure 8.5, the reason for this behavior is that vertical loading doesn't depend on viscosity of lubricant.

8.2 Affects of temperature variation from 40˚C to 95˚C at 1000 RPM

As the camshaft speed increases to 1000 rpm, the entraining velocity increases and so the minimum film thickness increases in comparison to 400 rpm. At 40˚ C the minimum film thickness at the flanks 6 µm indicating that at flanks there is hydrodynamic lubrication as shown in figure 8.8, and so the tappet friction and rotation is less at flanks as shown in figure 8.10.At cam nose the film thickness is .4 µm indicating that there is boundary lubrication present due to which friction increases and also tappet rotation increases, as shown in figures 8.8, 8.10 and 8.11.At 95˚ C and 1000 rpm, the minimum film thickness, shear friction and tappet rotation shows nearly the same behavior as at 95˚C and 400 rpm.

8.3 Affects of changing cam shaft speed from 400 rpm to 1000 rpm at 40˚C and 95˚C

As the camshaft speed increase from 400 to 1000 rpm, the minimum film thickness increases due to the reason that entraining velocity increases, as shown in figure 8.12. The vertical loading increases as the inertia increases at high camshaft speeds. At the flanks, at 1000 rpm due to inertia, the loading is greater in comparison to 400 rpm, but at the nose the vertical loading is less at the speed of 1000 rpm, because of the reason that loading decreases as the acceleration of tappet decreases at the nose region, as shown in figure 8.13. At 1000 rpm, cam tappet friction also increases at the flanks but decreases at the nose in comparison to 400 rpm, same goes for tappet rotation, as shown in figure 8.14 and 8.15. The reason for this kind of behavior is that at 1000 rpm, friction depends on vertical loading. As the temperature increases the minimum film thickness decreases at the flanks and at the nose as shown in figure 8.16.The values of shear friction and tappet rotation at 400 rpm and 95˚ C decreases in comparison to 40˚ C, but the profile of graphs remains same, as shown in figures 8.17 and 8.18. At 1000 rpm and 95˚C, the friction depends on vertical loading, that's why the temperature change doesn't affect the values of shear friction and tappet rotation as shown in figures 8.17 and 8.18.

8.4 Affects of friction Modifier at camshaft speeds 400 rpm and 1000 rpm at limiting coefficients .08 and .12:

The affects of friction modifiers can only be seen above 80˚C, so in this portion of parametric study temperature is held at 95˚C. Friction modifier doesn't affect the minimum film thickness

as shown in figure 8.19. Vertical loading is also not affected by changing limiting coefficient of friction, as shown in figure 8.20. As shear friction cannot be greater than limiting value of friction which depends on limiting coefficient of friction and increases with increasing limiting coefficient so the shearing friction increases as shown in figure 8.21.Tappet rotation also increases with increasing limiting coefficient as friction increases, as shown in figure 8.22.At 1000 rpm similar kind of behavior can be seen in figures 8.23, 8.24, 8.25 and 8.26.

8.5 Affects of surface roughness at 400 rpm and 1000 rpm, 40˚C and 95˚C:

With and without surface roughness there is no change in minimum film thickness and vertical loading as shown in the figures 8.27, 8.28, 8.30, 8.31, 8.33, 8.34, 8.36 and 8.37. Due to surface roughness there is change in shear friction at the cam nose because at the cam nose there is boundary lubrication regime and asperities are in contact with each other so the friction increases, as shown in figures 8.29, 8.32, 8.35 and 8.38.

8.6 Affects of Tappet Rotation at 400 rpm to 1000 rpm speed and 95˚C temperature:

At 400 rpm and 95˚C with tappet rotation the minimum film thickness is greater at flanks and nose in comparison to non rotating tappet, the reason is that velocity of contact point with respect to tappet has an additional component to incorporate tappet rotation and so the entraining velocity is greater if tappet is rotating. As minimum film thickness is dependent on entraining velocity so it increases, as shown in figure 8.39. Figure 8.40 shows that the friction decreases due to tappet rotation as the sliding velocity increases. At 1000 rpm the behavior is similar as for 400 rpm, shown in figures 8.41 and 8.42.

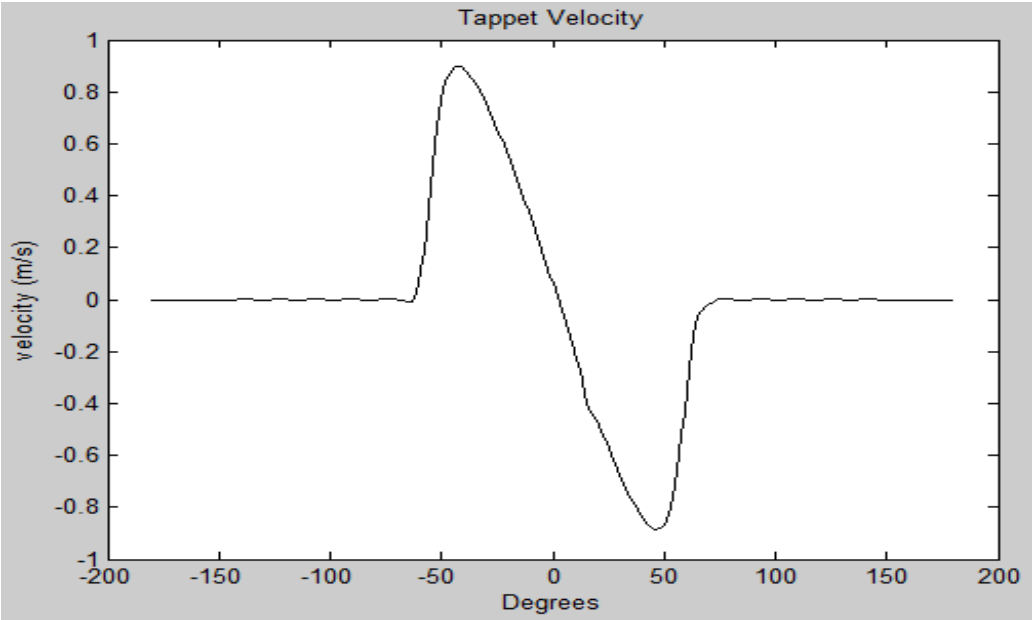

Figure 8.1 Tappet Velocity

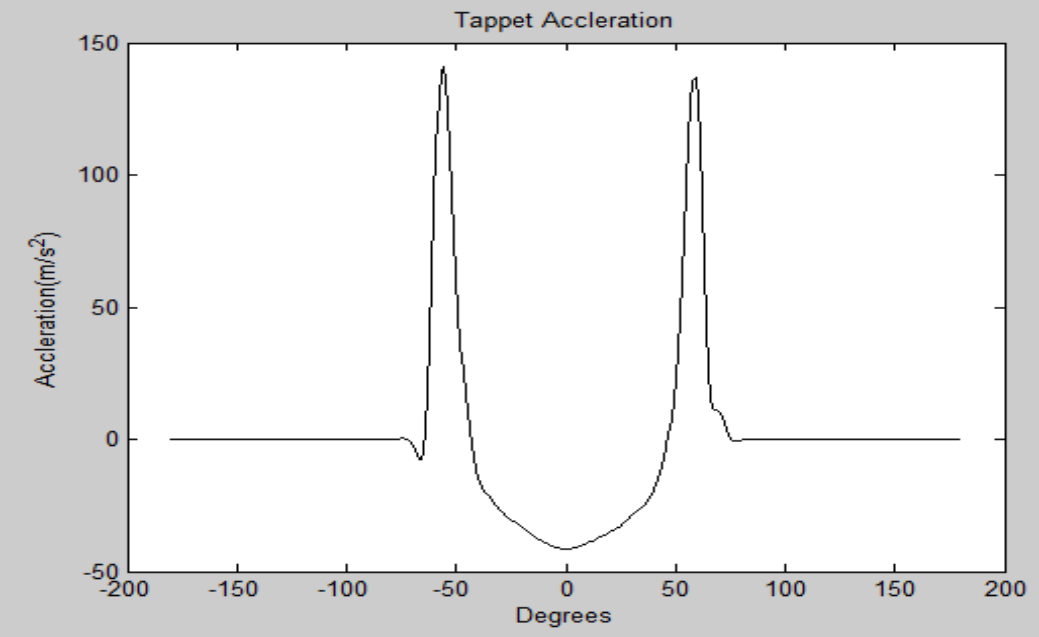

Figure 8.2 Tappet Acceleration

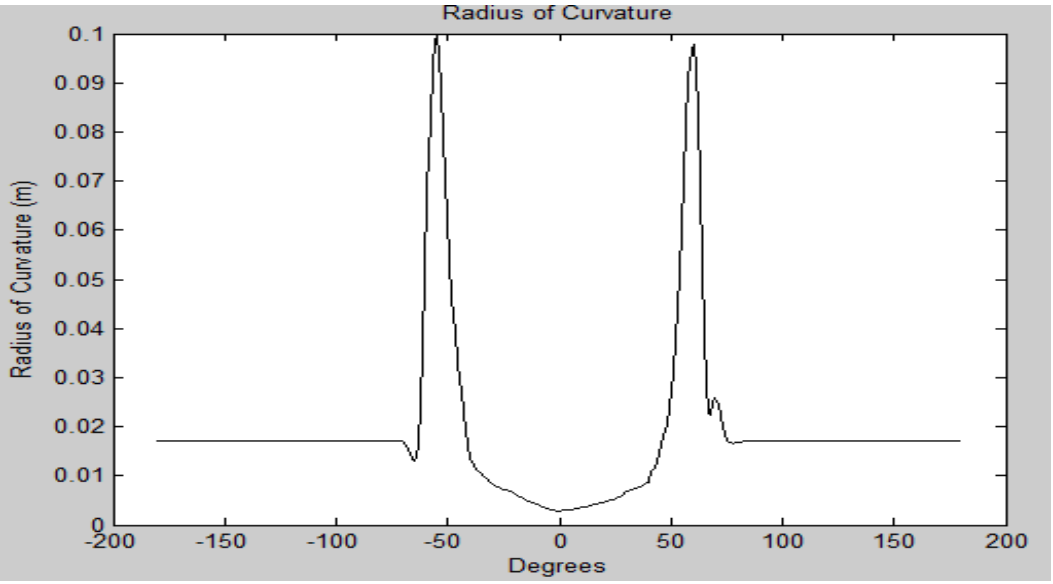

Figure 8.3 Radius of Curvature

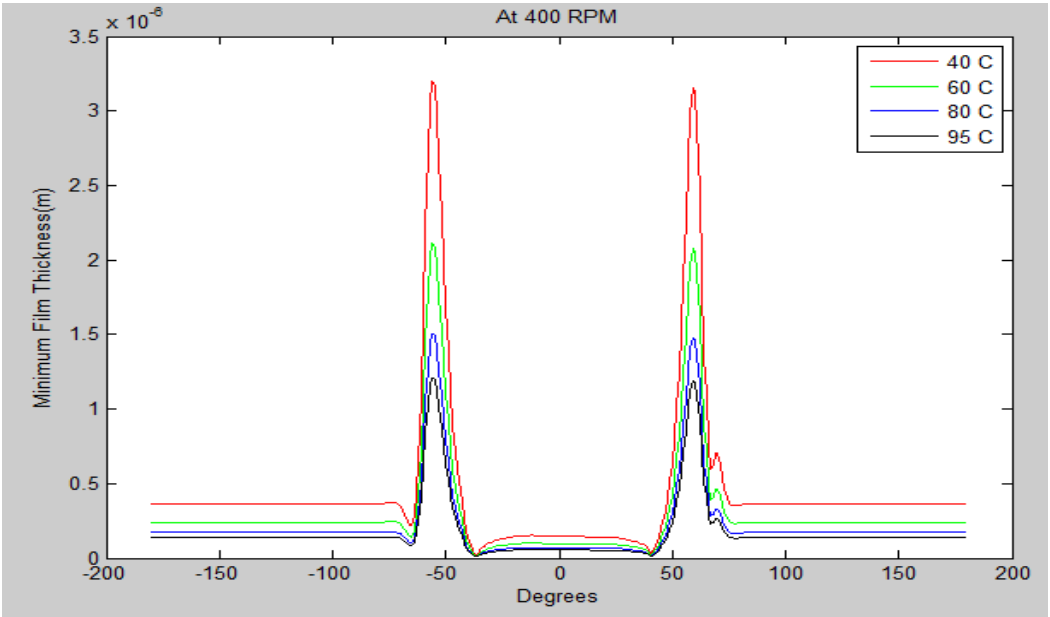

Figure 8.4 Minimum film thicknesses at 400 rpm and different temperatures

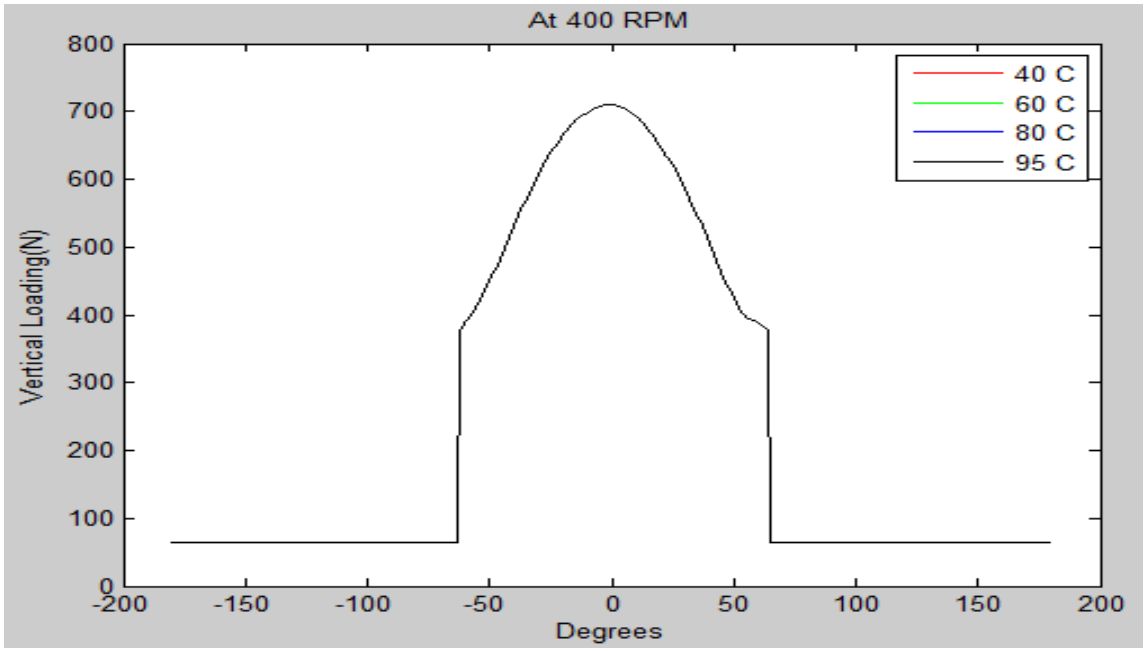

Figure 8.5 Vertical loading at 400 rpm and different temperatures

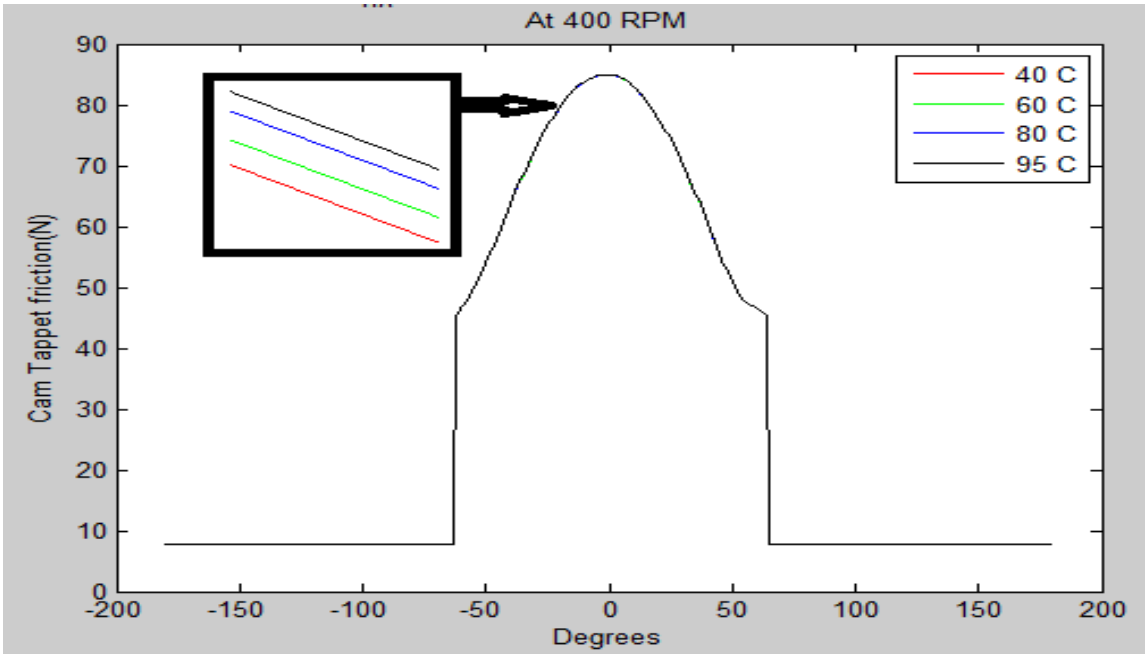

Figure 8.6 Cam/Tappet shear frication at 400 rpm and different temperatures

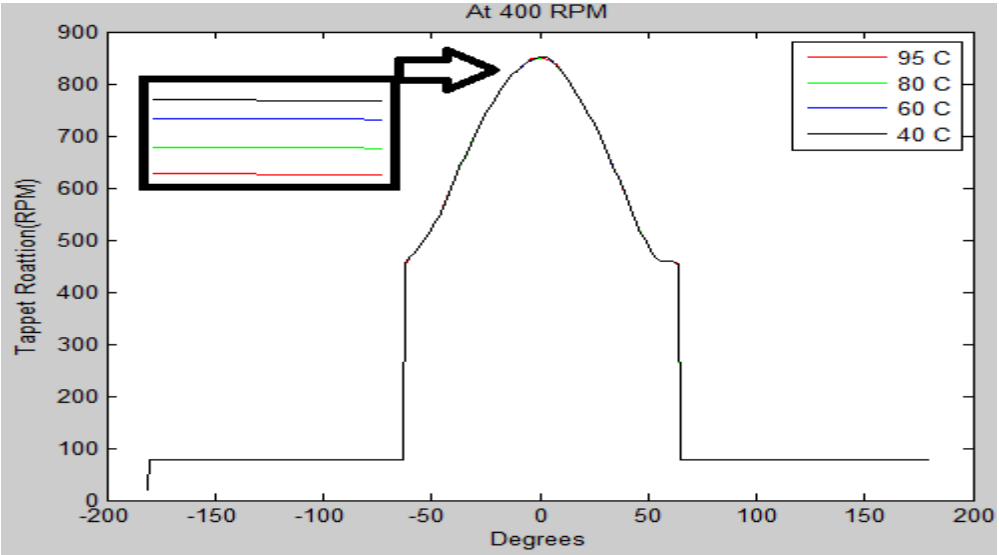

Figure 8.7 Tappet Rotation at 400 rpm and different temperatures

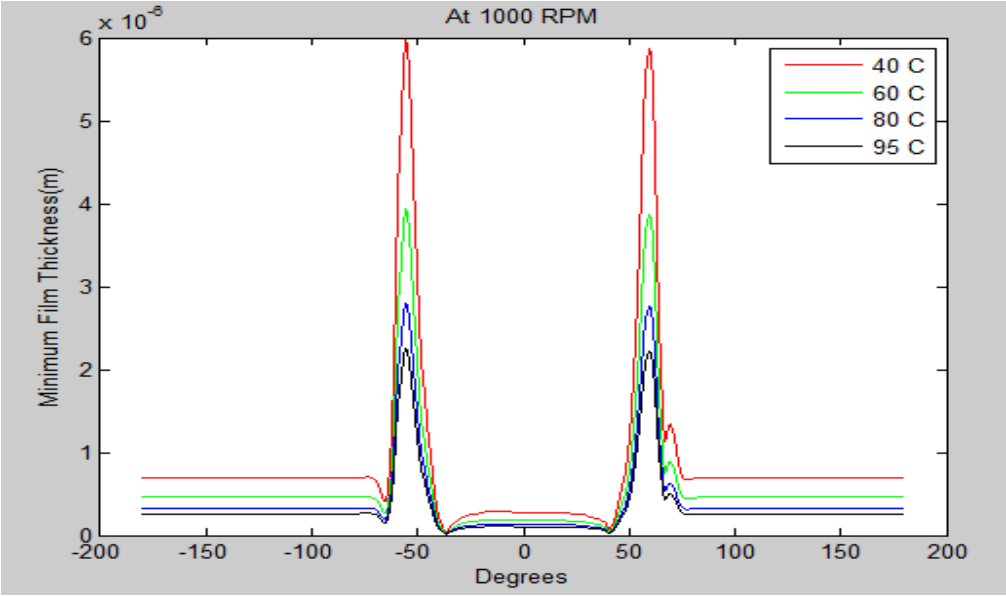

Figure 8.8 Minimum film thicknesses at 1000 rpm and different temperatures

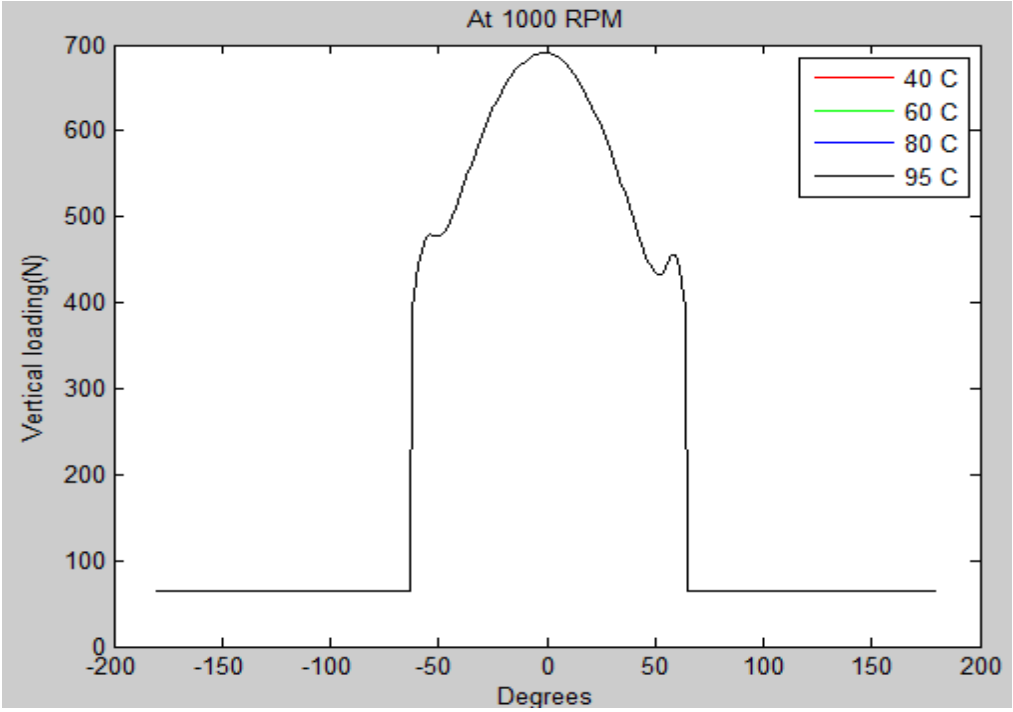

Figure 8.9 Vertical loading at 1000 rpm and different temperatures

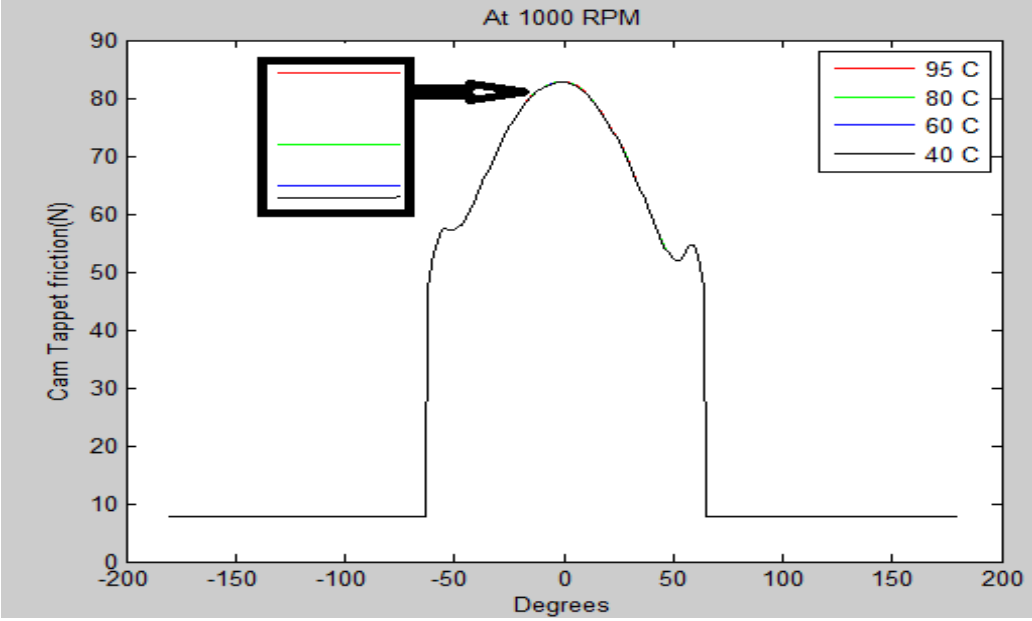

Figure 8.10 Cam/Tappet frictions at 1000 rpm and different temperature

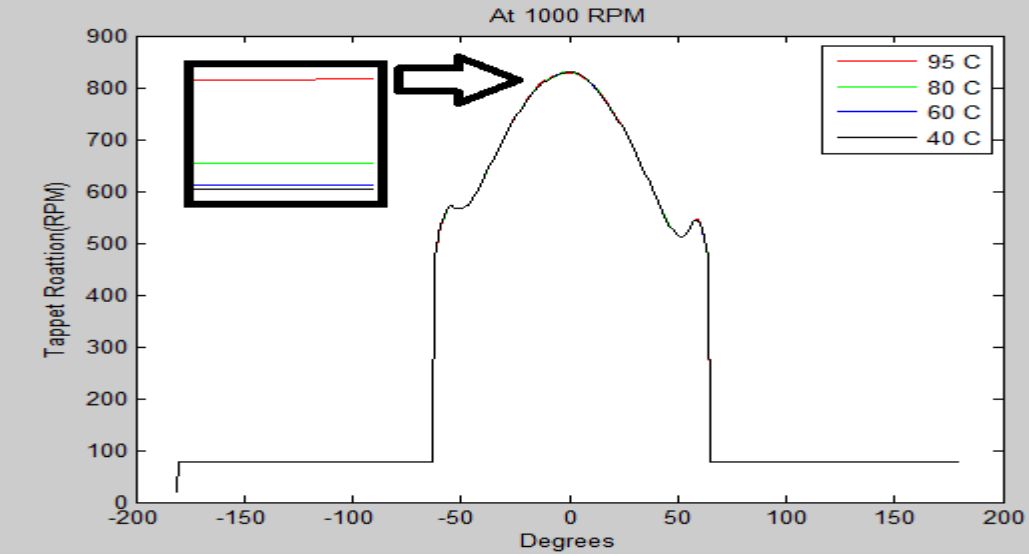

Figure 8.11 Tappet rotation at 1000 rpm and different temperatures

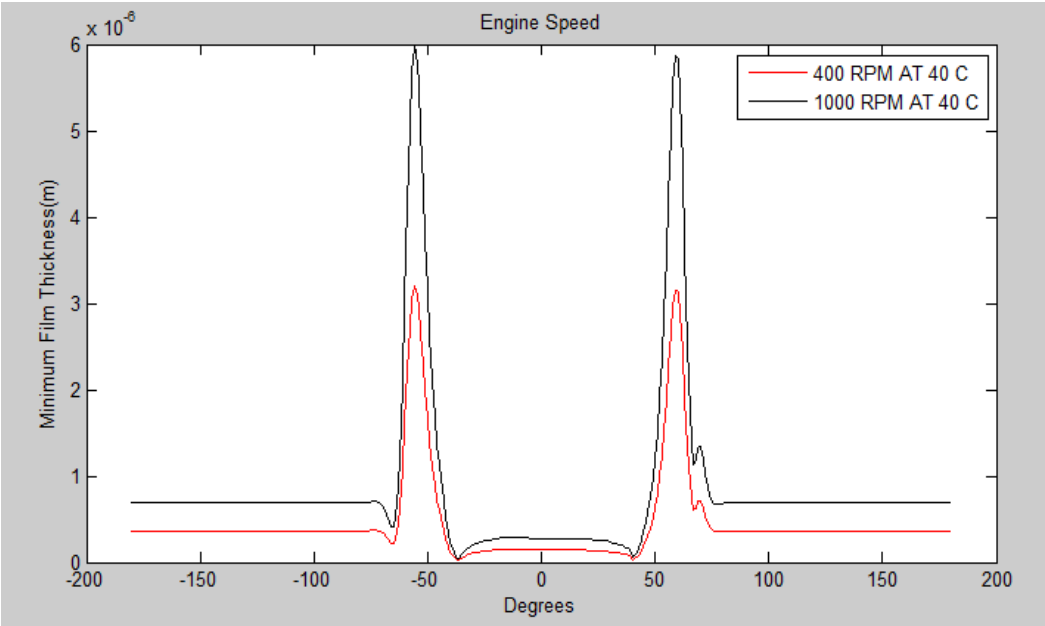

Figure 8.12 Minimum film thicknesses at 40 C, 400 rpm and 1000 rpm

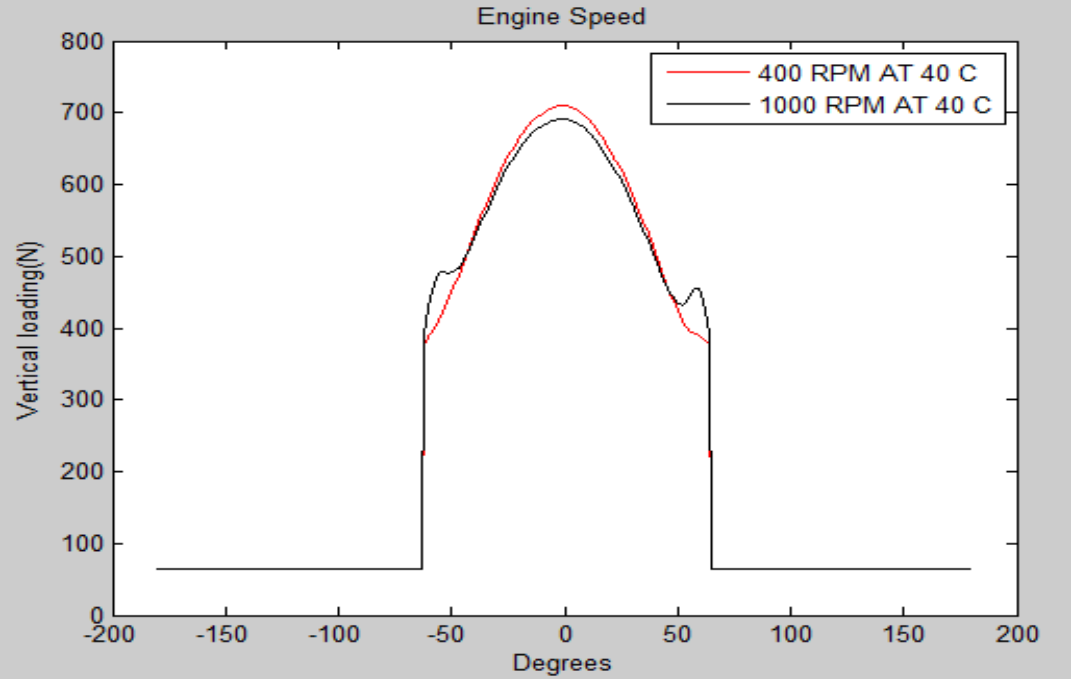

Figure 8.13 Vertical loading at 40 C, 400 rpm and 1000 rpm

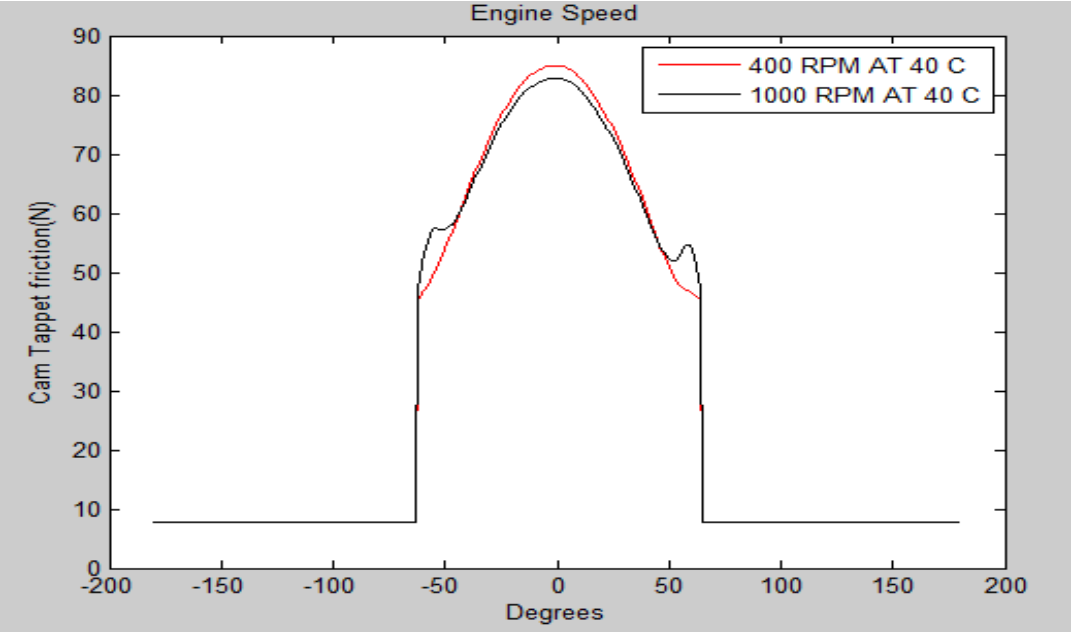

Figure 8.14 Cam/Tappet friction at 40 C, 400 rpm and 1000 rpm

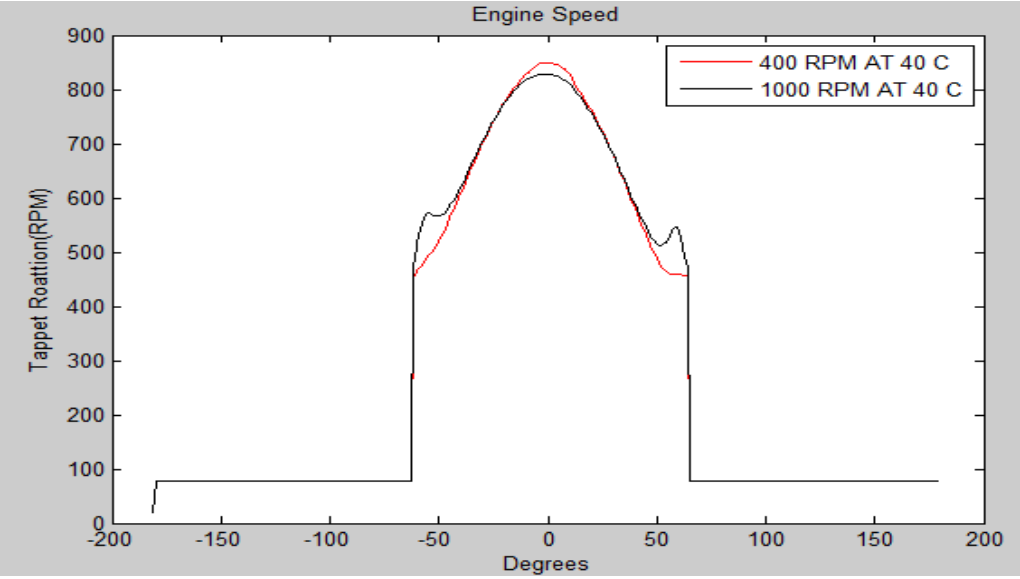

Figure 8.15 Tappet rotation at 40 C, 400 rpm and 1000 rpm

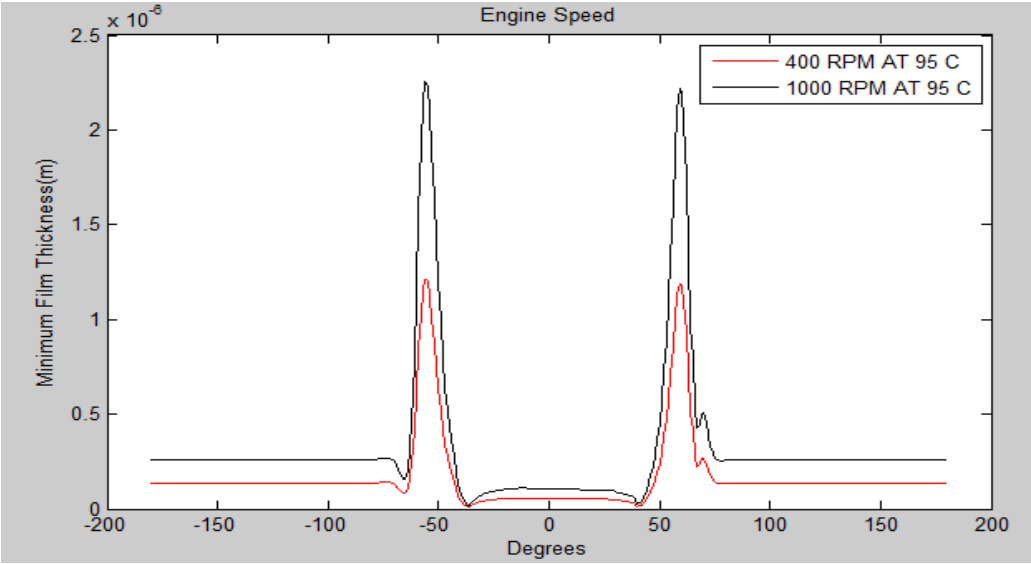

Figure 8.16 Minimum film thicknesses at 95 C, 400 rpm and 1000 rpm

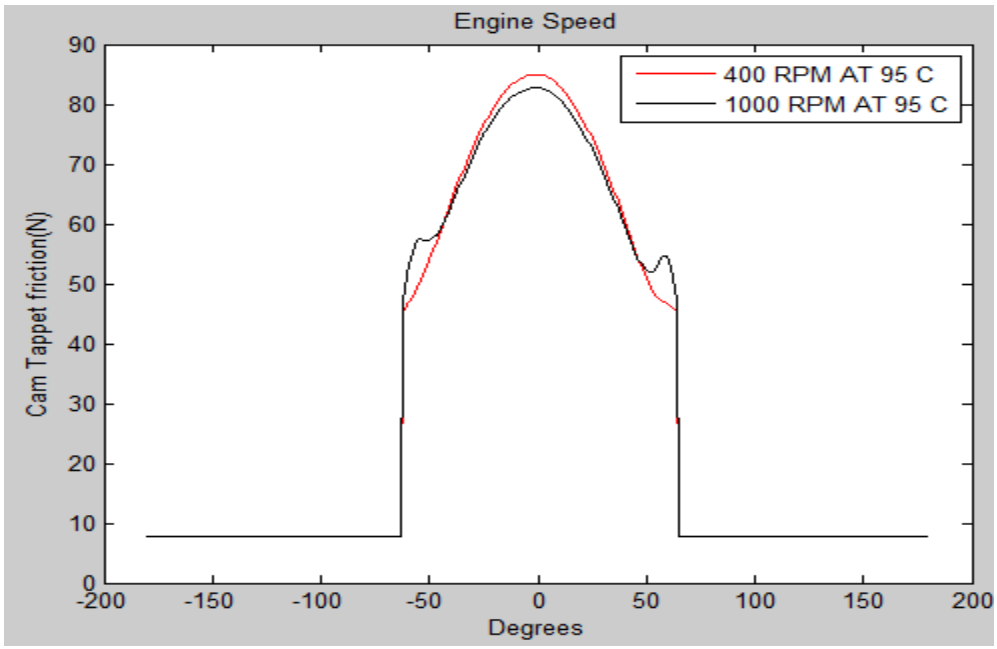

Figure 8.17 Cam/Tappet friction at 95 C, 400 rpm and 1000 rpm

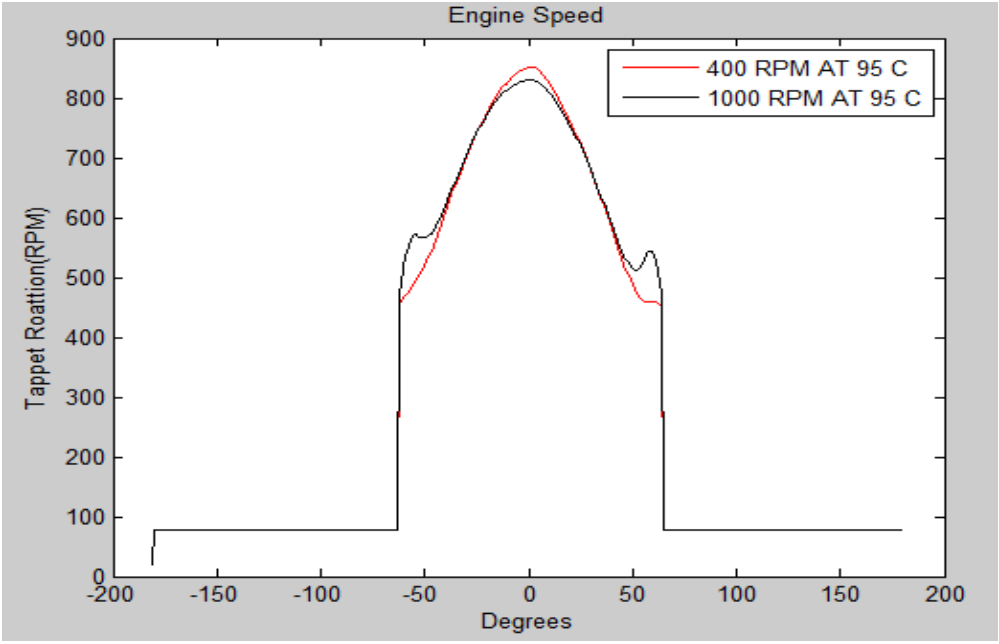

Figure 8.18 Tappet rotation at 95 C, 400 rpm and 1000 rpm

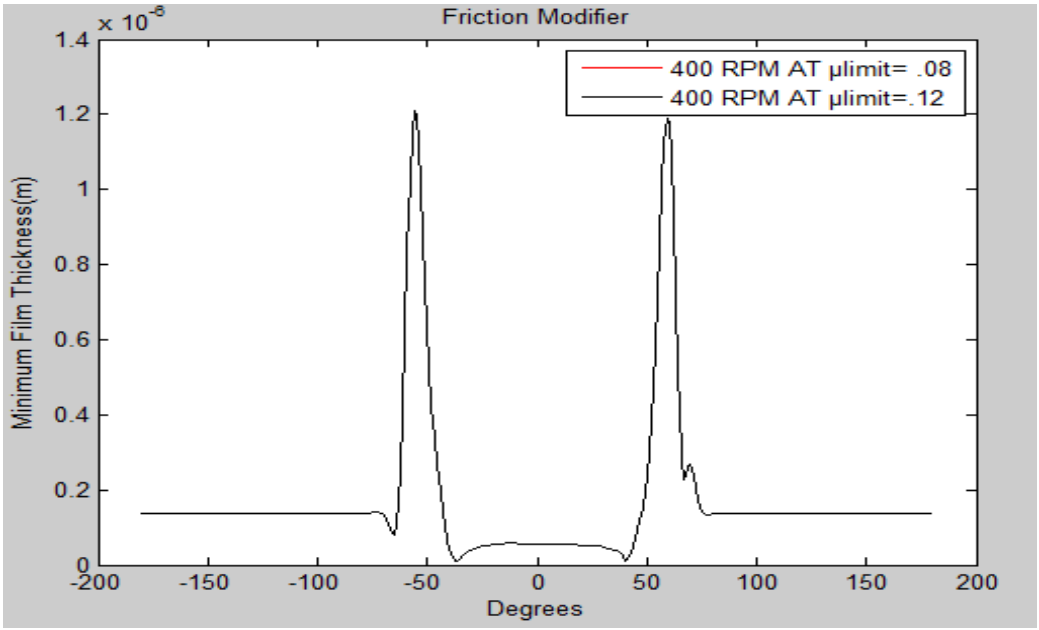

Figure 8.19 Minimum film thickness at 95 C, 400 rpm and

different limiting coefficients

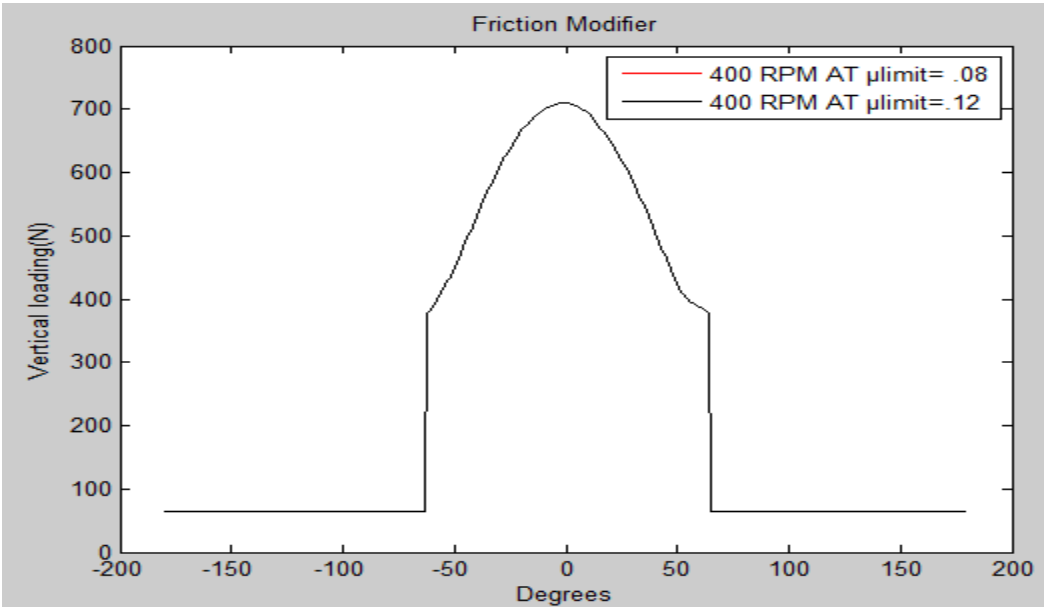

Figure 8.20 Vertical loading at 95 C, 400 rpm and different

limiting coefficients of friction

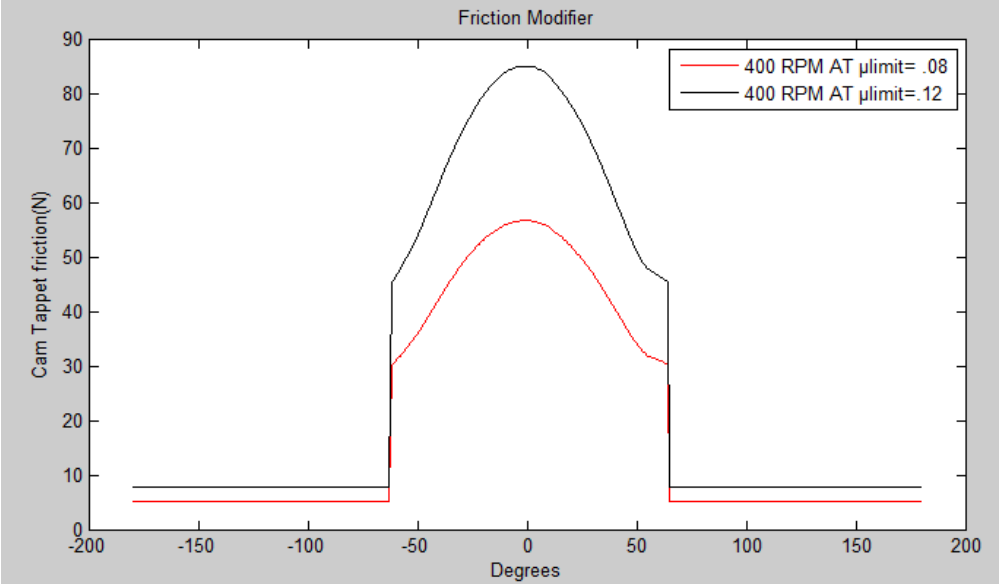

Figure 8.21 Cam/Tappet friction at 95 C, 400 rpm and different limiting coefficients of friction

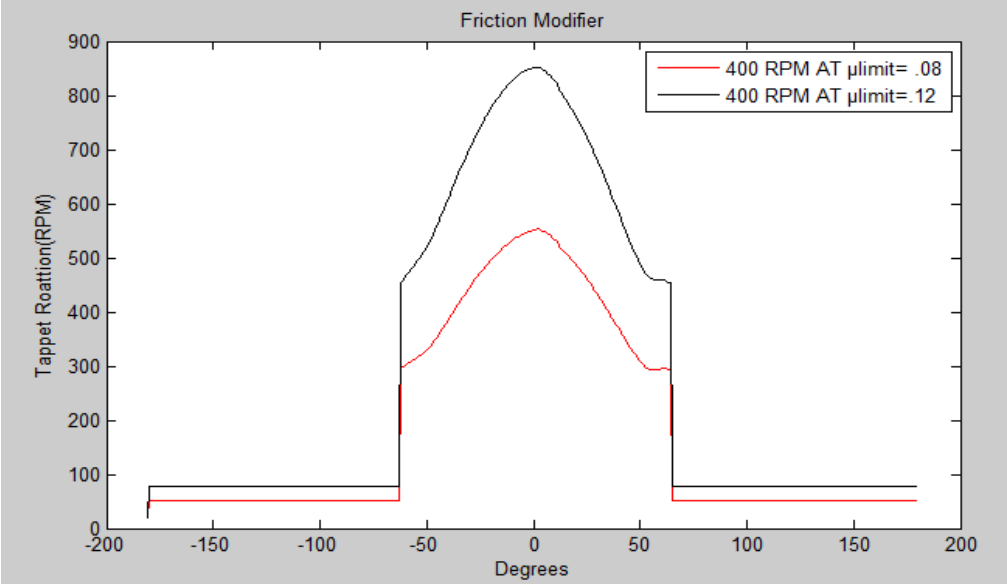

Figure 8.22 Tappet rotation at 95 C, 400 rpm and different limiting coefficients of friction

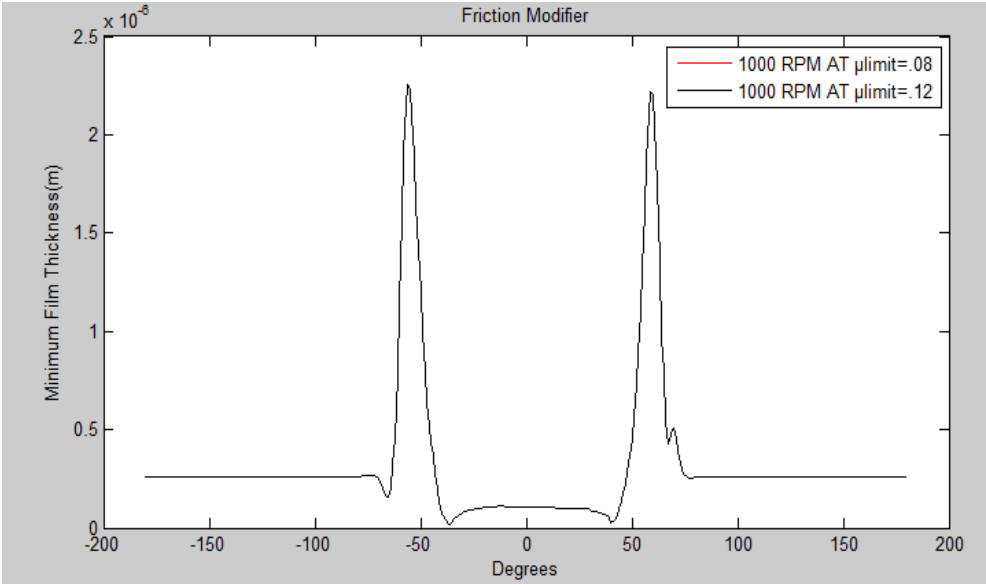

Figure 8.23 Minimum film thicknesses at 95 C, 1000 rpm and different limiting coefficients

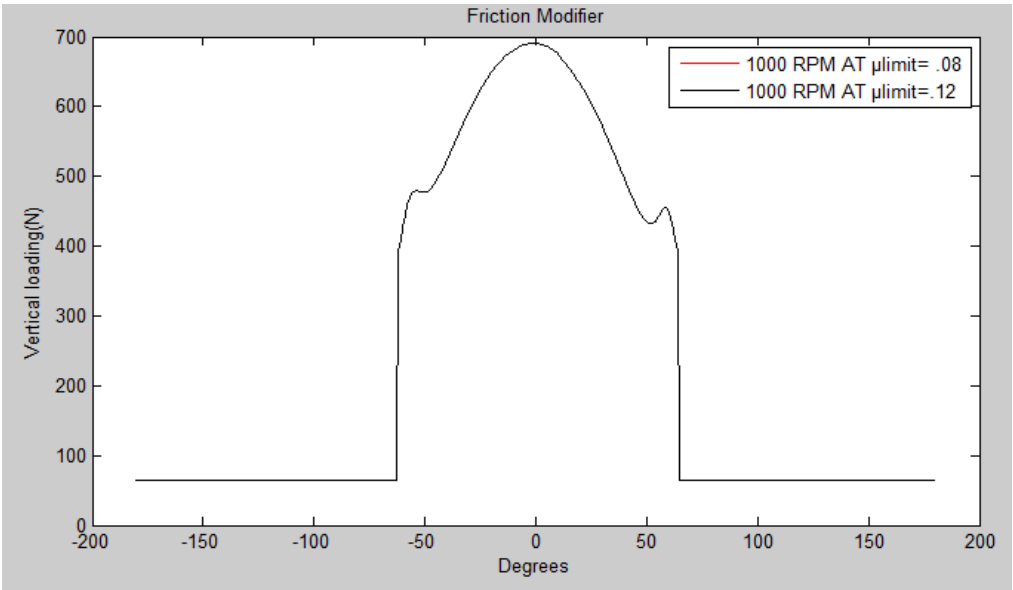

Figure 8.24 Vertical loading at 95 C, 1000 rpm and different limiting coefficients of friction

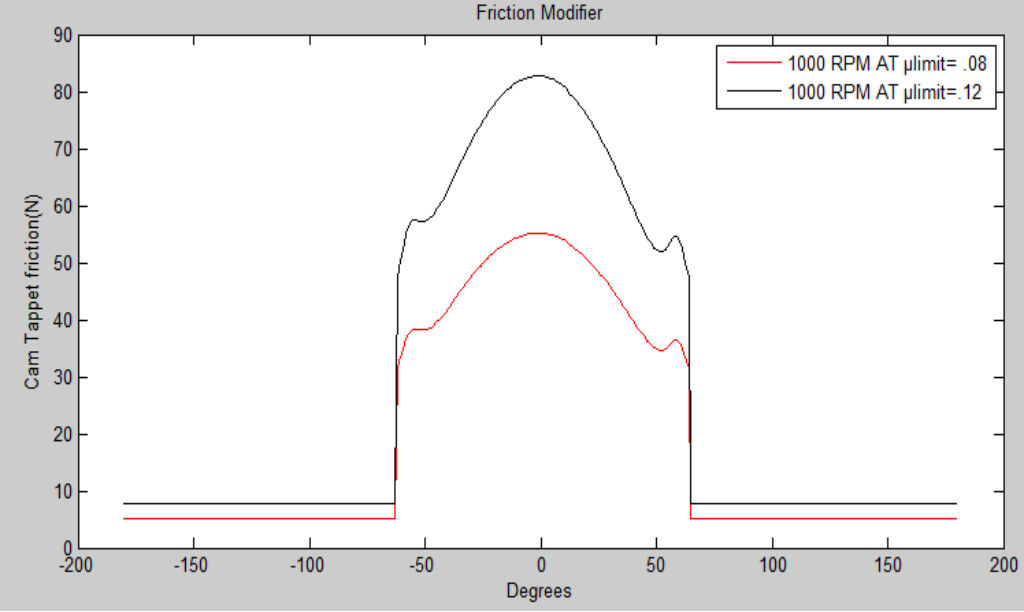

Figure 8.25 Cam/Tappet friction at 95 C, 1000 rpm and different limiting coefficients of friction

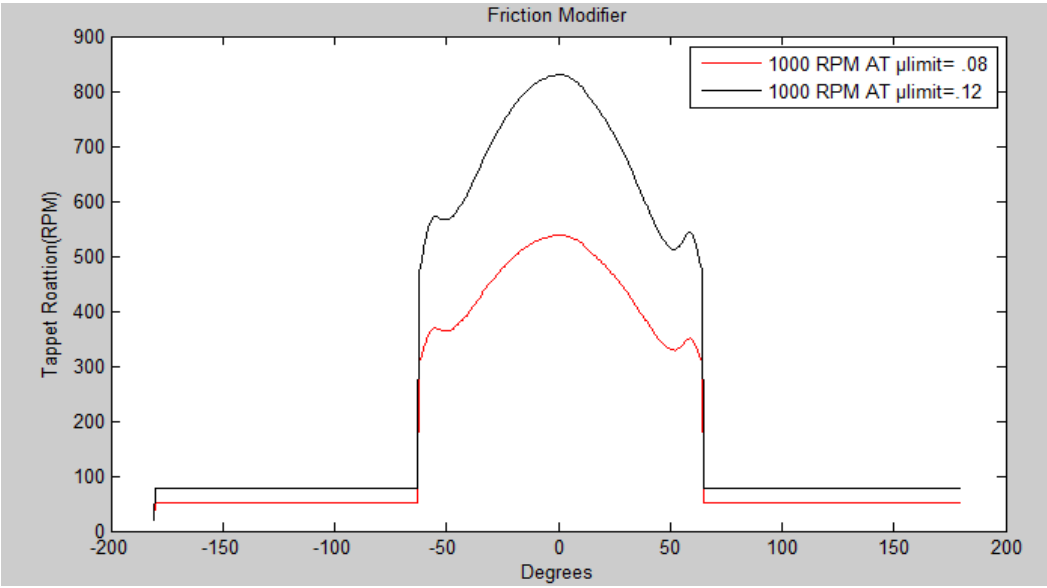

Figure 8.26 Tappet rotation at 95 C, 1000 rpm and different limiting coefficients of friction

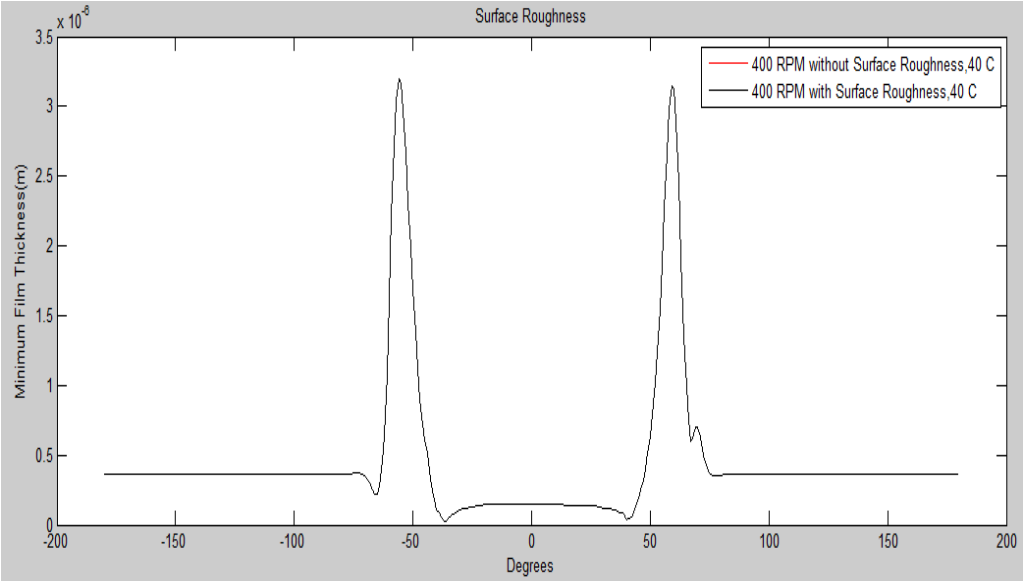

Figure 8.27 Minimum film thicknesses with and without

surface roughness at 400 rpm and 40 C

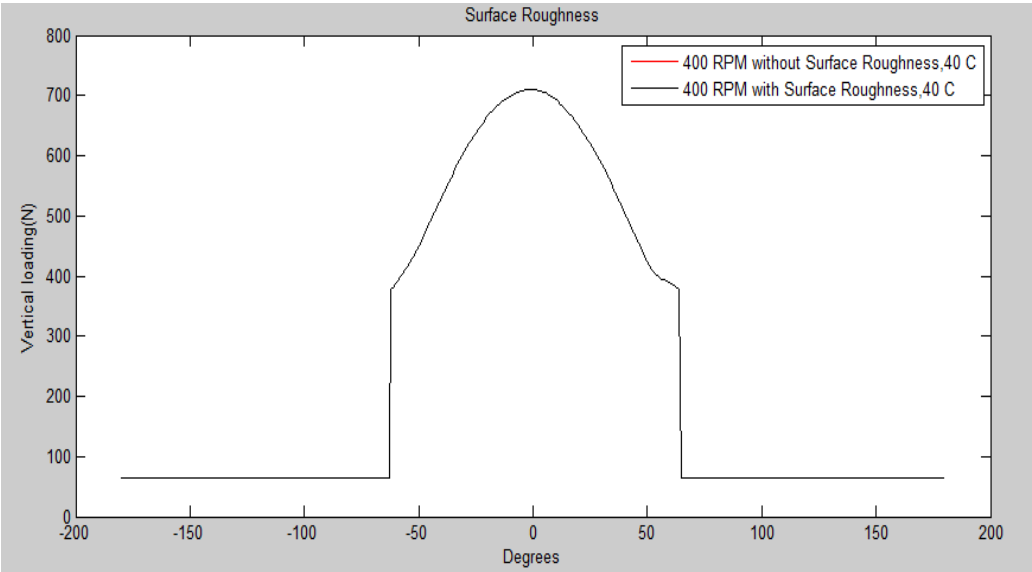

Figure 8.28 Vertical loading with and without

surface roughness at 400 rpm and 40 C

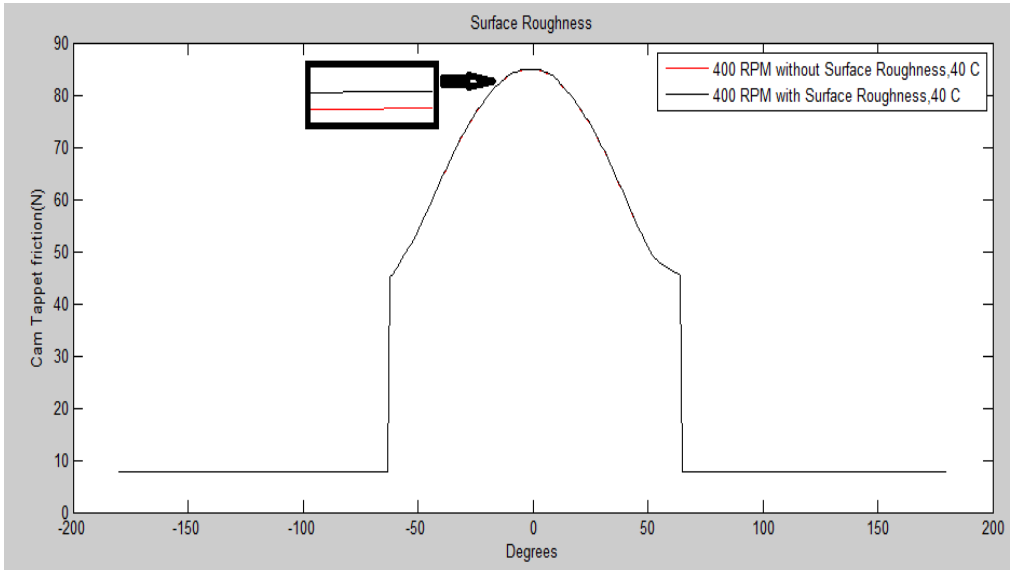

Figure 8.29 Cam/Tappet friction with and without

surface roughness at 400 rpm and 40 C

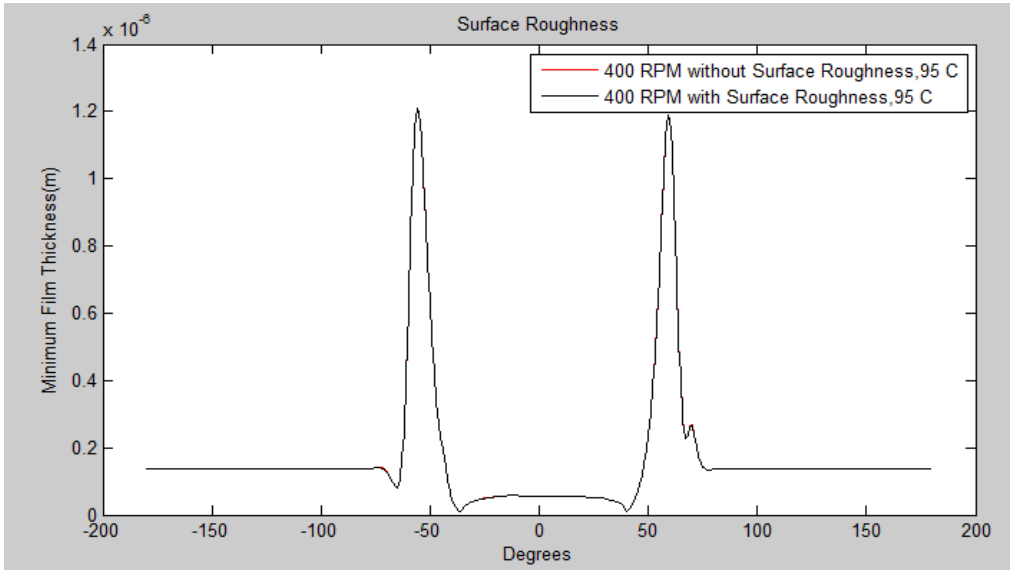

Figure 8.30 Minimum film thicknesses with and without

surface roughness at 400 rpm and 95 C

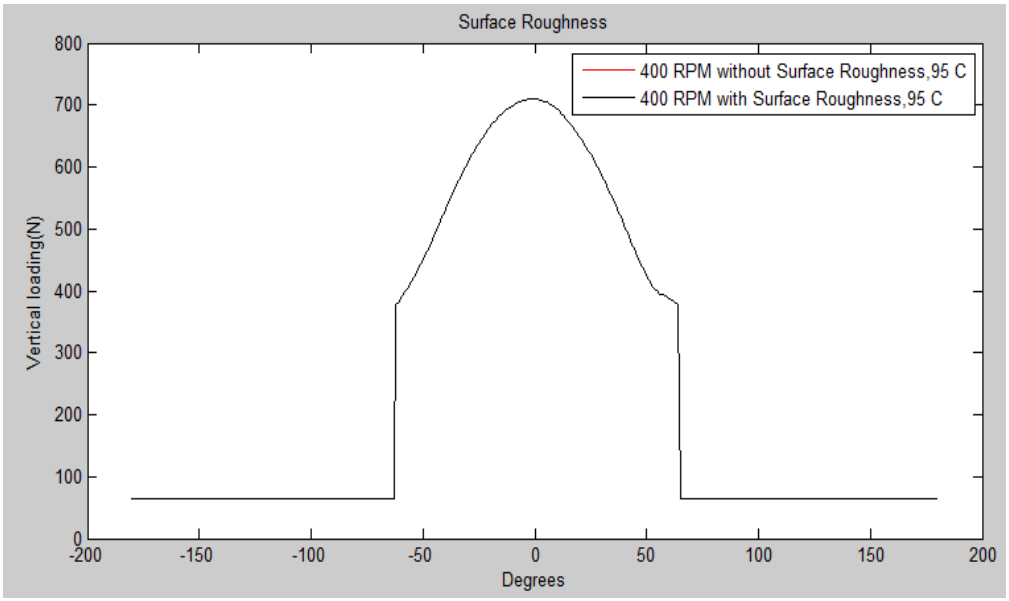

Figure 8.31 Vertical loading with and without

surface roughness at 400 rpm and 95 C

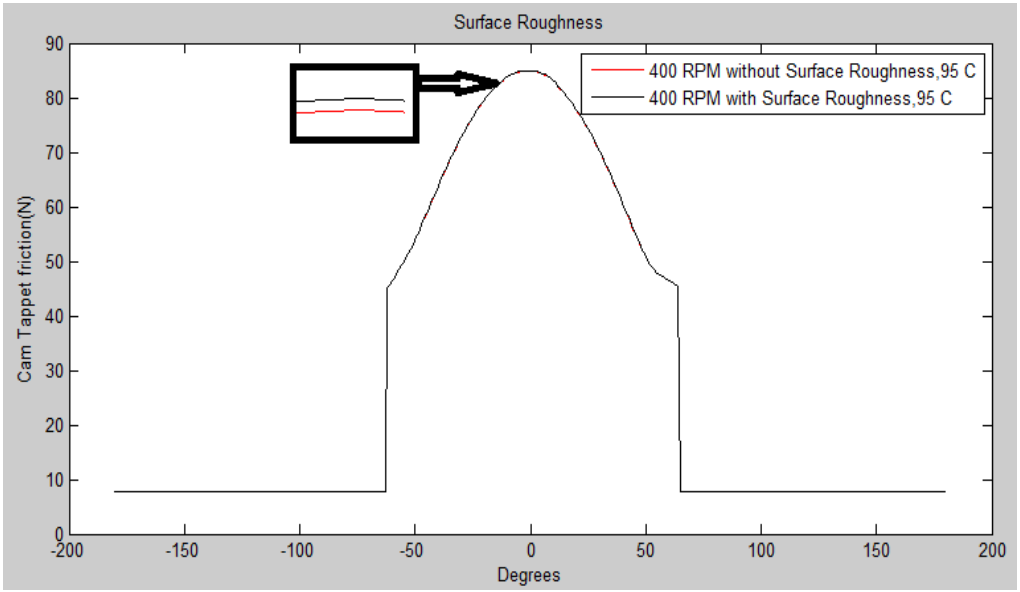

Figure 8.32 Cam/Tappet friction with and without

surface roughness at 400 rpm and 95 C

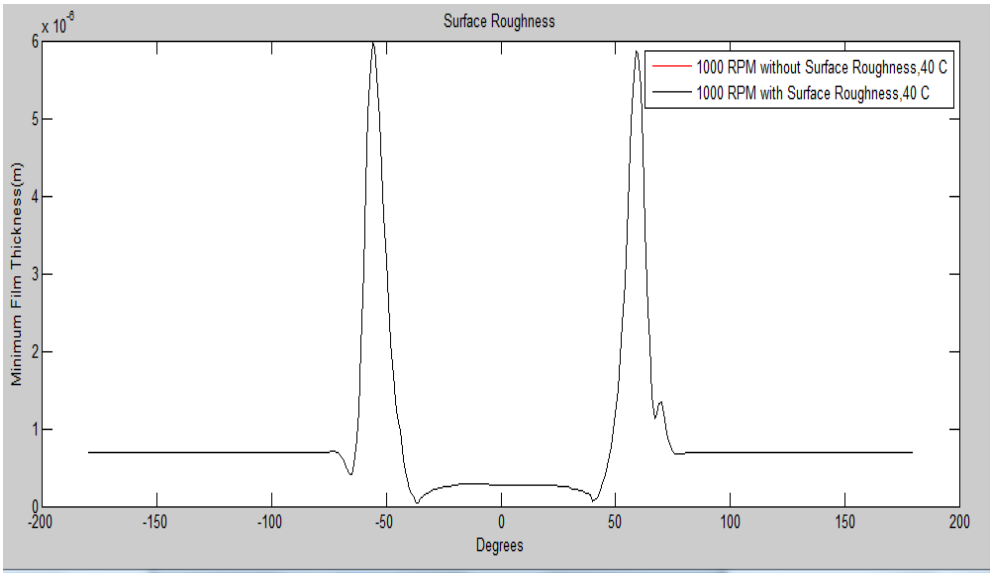

Figure 8.33 Minimum film thickness with and without

surface roughness at 1000 rpm and 40 C

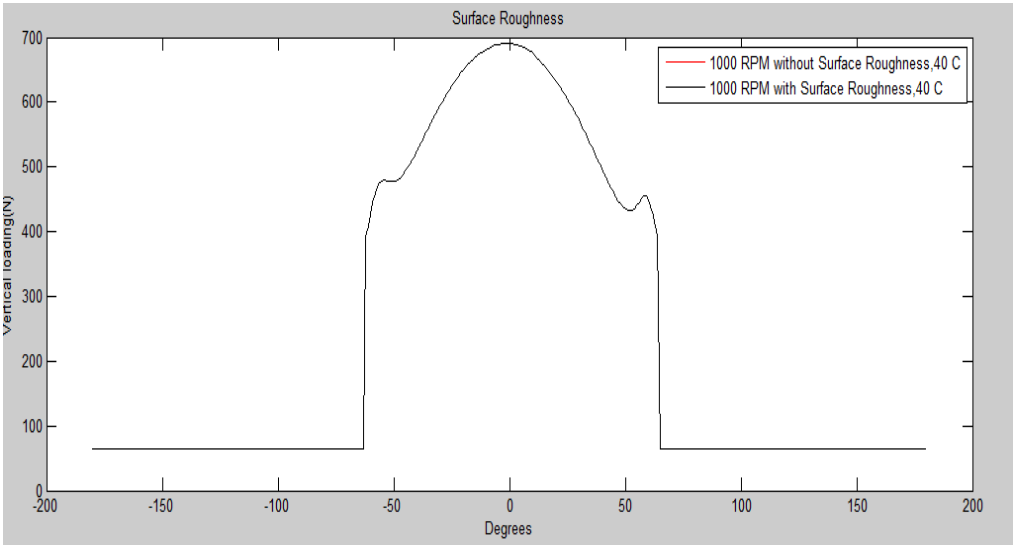

Figure 8.34 Vertical loading with and without

surface roughness at 1000 rpm and 40 C

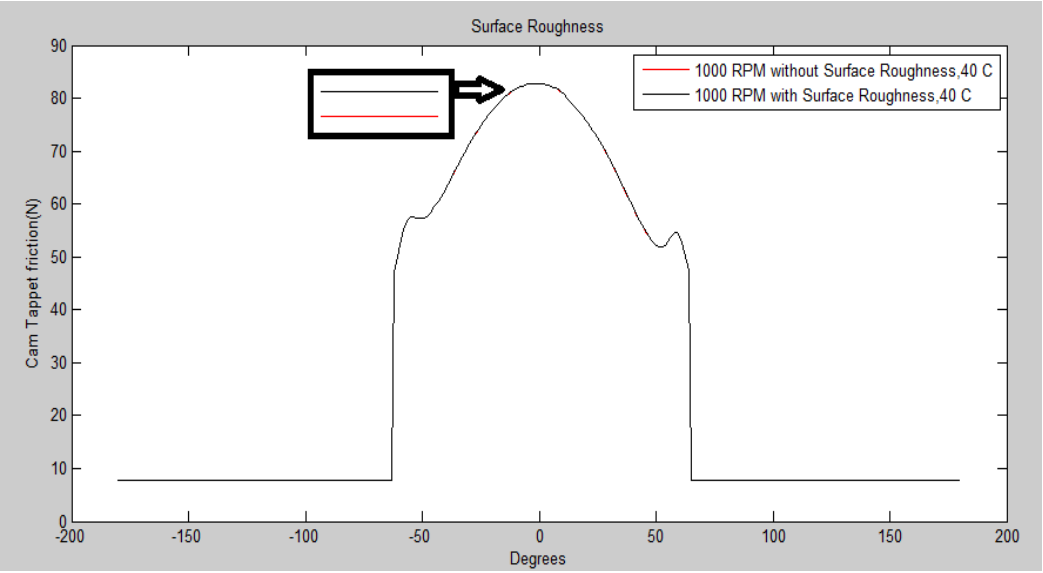

Figure 8.35 Cam/Tappet friction with and without

surface roughness at 1000 rpm and 40 C

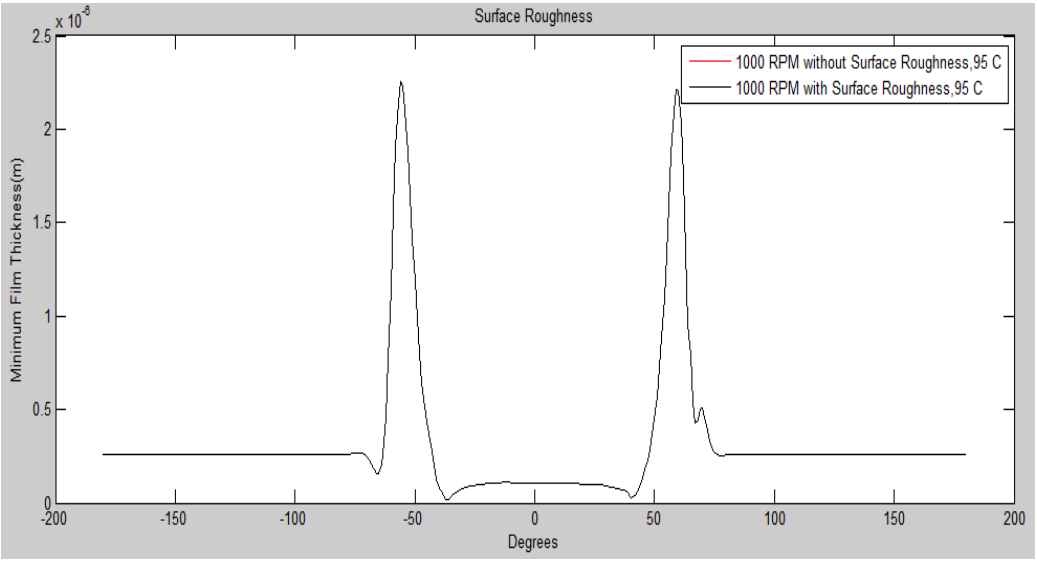

Figure 8.36 Minimum film thickness with and without

surface roughness at 1000 rpm and 95 C

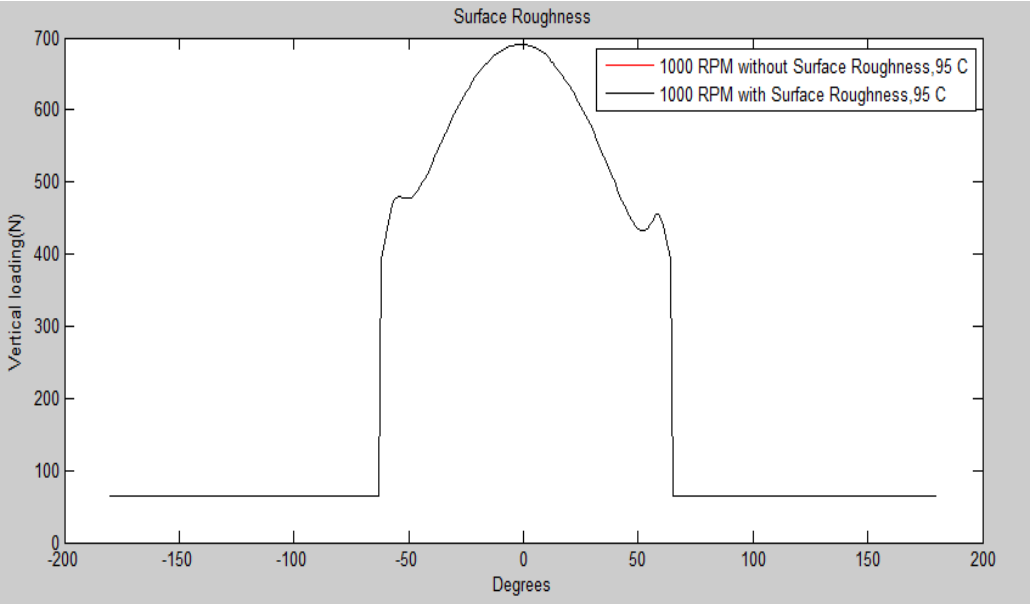

Figure 8.37 Vertical loading with and without surface

roughness at 1000 rpm and 95 C

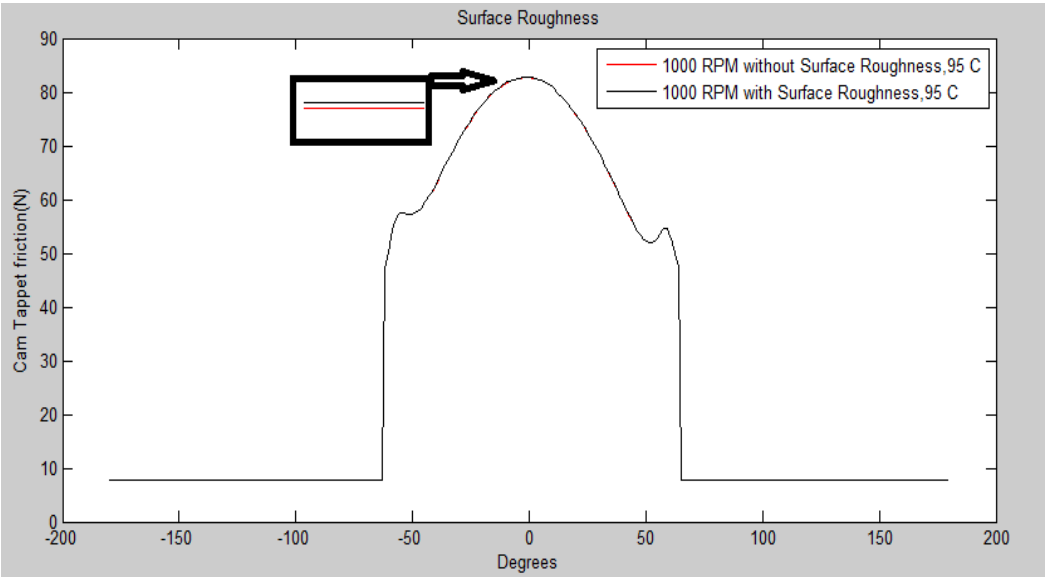

Figure 8.38 Cam/tappet friction with and without surface

roughness at 1000 rpm and 95 C

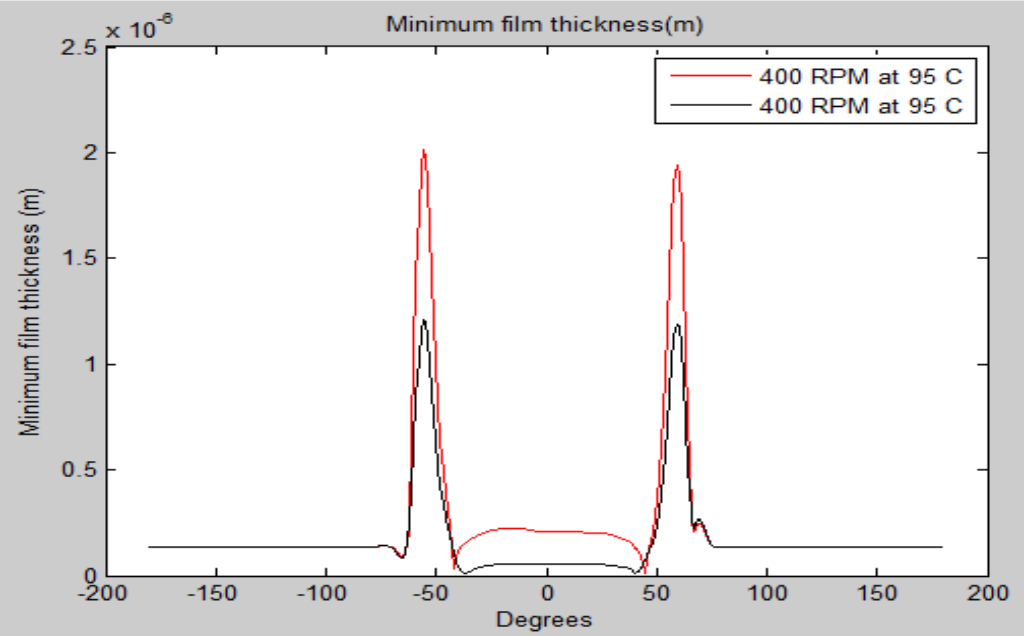

Figure 8.39 Minimum film thickness with and without

rotation at 400 rpm and 95C

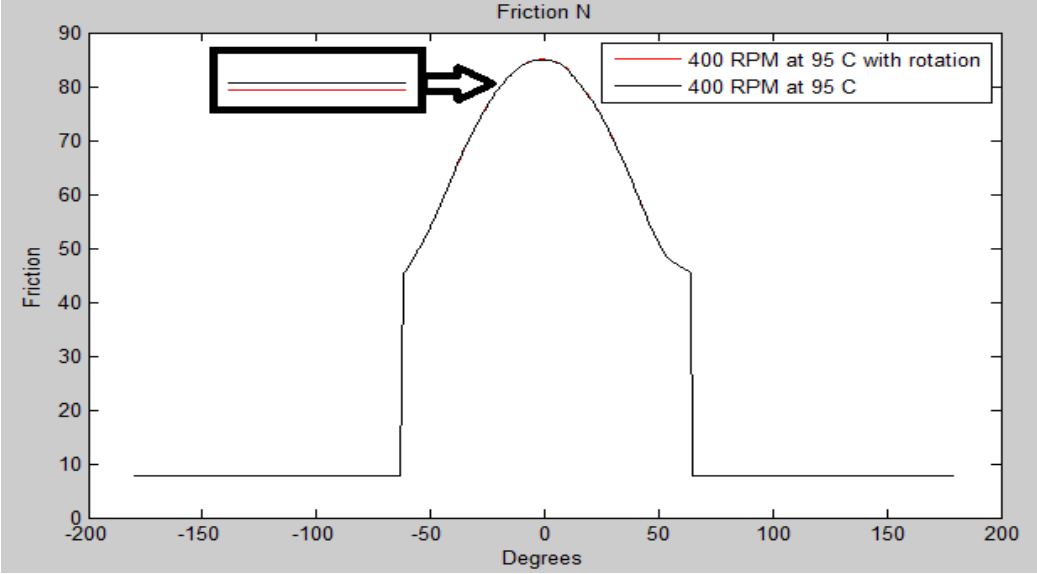

Figure 8.40 Cam/tappet friction with and without rotation at 400 rpm and 95C

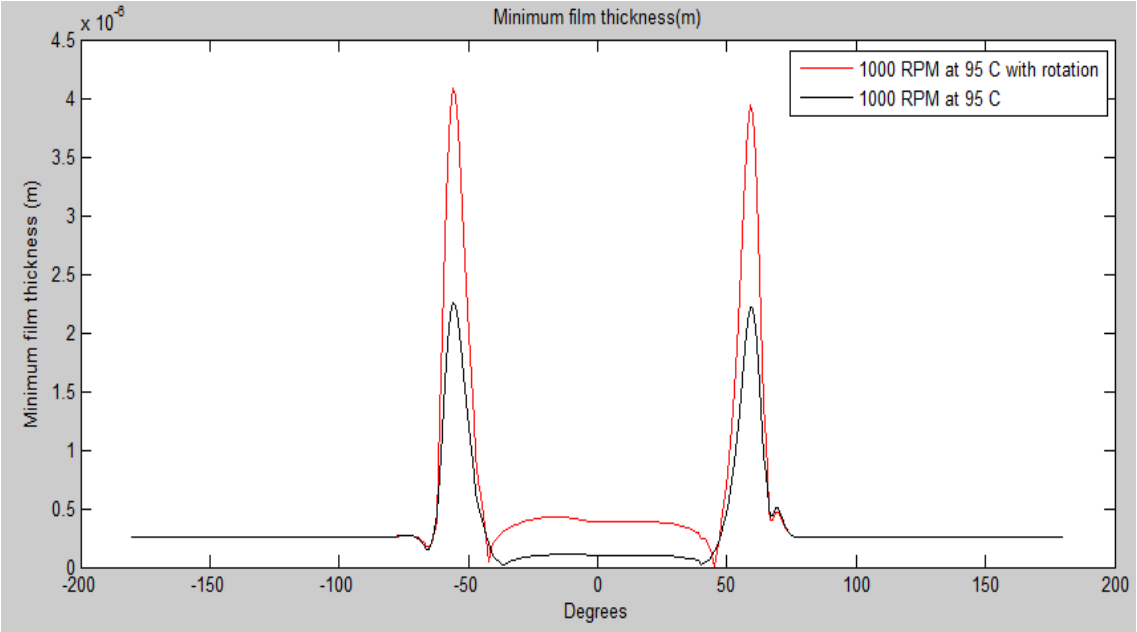

Figure 8.41 Minimum film thickness with and without

rotation at 1000 rpm and 95C

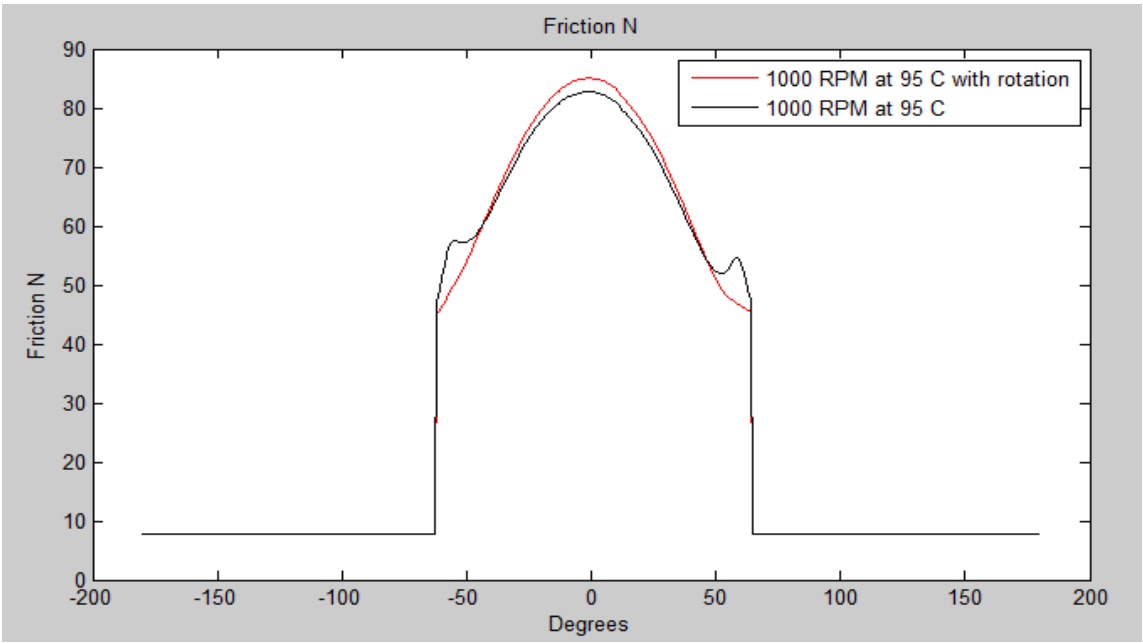

Figure 8.42 Friction with and without rotation at 1000 rpm and 95C

Conclusions

- As the camshaft speed increases, the minimum film thickness increases due to the increase in entraining velocity
- Due to the tappet rotation, the minimum film thickness increases and friction reduces.
- Shear friction depends upon limiting value of friction due to the inaccuracies of Baraus equation.
- If surface roughness effects are included in the model then the overall friction increases due to the asperities coming into contact with each other. The rise in overall friction is small as compared to shear friction at the cam/tappet contact
- Power loss increases, if the friction between the tappet/bore contact is included in the overall friction.
- At the cam flanks the hydrodynamic lubrication is present at low speeds. As the speed increases EHL regime is formed. At the nose region the lubrication regimes varies between mixed and boundary lubrication.

Future Work

- Few changes in this model can be made to use it for domed shape tappets.
- Comparison between different valve train types will be an interesting study.
- Baraus equation used to find the lubricant viscosity at different pressures doesn't give optimum results at high pressure, so other methods should be used to find the lubricant's viscosity.
- Parametric studies can be done to find the optimum parameters for designing cam shape like cam base circle and nose radius etc.

References

[1] Ball A D, Dowson D and Taylor C M 1989, 'Cam and Follower Design', of 15th Leeds-Lyon Symposium on Tribology - Tribological Design of Machine Elements, Buttenvorths, pp 1 1-1 30.

[2] Buuck B A, 1982, 'Elementary Design Considerations for Valve Gears', *SAE* 821574

[3] Crane, M.E. and Meyer, R.C. 1990, 'A Process to Predict Friction in an Automotive Valve Train', *SAE* 901728.

[4] Choi, J.K., Min, B.S. and Oh, D.Y. 1995, 'A Study on the Friction Characteristics of Engine Bearings and Cam/Tappet Contacts from the Measurement of Temperature and Oil Film Thickness', *SAE* 952472.

[5] Dyson, A. and Naylor, 11. 1961, 'Application of the flash temperature concept to Cam and Tappet wear problems', *Proc. Instn. Mech. Engrs.,* Vol. 175, No. 8, pp.255-280.

[6] Dowson D, Taylor C. M. and Zhu G 1991, 'A Transient Elastrohydrodynamic Lubrication Analysis of Cam and Follower', Frontiers of Tribology Conference IOP. *To be published in Journal of Physics D: Applied Physics*

[7] Dowson, D., Taylor, C.M. and Zhu, G. 1986, 'Mixed lubrication of a cam and flat faced follower', Proceedings, 13th Leeds-Lyon Symposium, Butterworths, pp.599-609.

[8] Dowson D, Harrison P and Taylor C M 1985, 'The Lubrication of Automotive Cams and Followers', Mechanisms and Surface Distress, 12th Leeds- Lyon Symposium on Tribology, pp 305-322, Butterworths.

[9] Dyson A and Naylor H 1960, 'Application of the Flash Temperature Contact to Cam and Tappet Wear Problems', *IMechE,* Proc Auto Div No 8, pp 225-280.

[10] Dowson D and Toyoda S 1979, 'A Central Film Thickness Formula for Elastrohydrodynamic Line Contacts', Elastrohydrodynamics and Related Topics, 5th Leeds-Lyon Symposium on Tribology, pp 60-65, MEP (IMECH)

[11] Evans, C.R. and Johanson, K. L. 1986, 'The Rheological properties of Elastrohydrodynamic Lubricant', *Proc. Instn Mech. Engrs. Part C* , 200 (5), 625 -633.

[12] Greenwood, J.A. and Tripp, J.H. 1970, 'The contact of two nominally flat rough surfaces', *Proc. Instn Mech. Engrs,* 185, 625-633.

[13] Gecim, B.A. 1992, 'Tribological study of a low friction Cam/Tappet system including tappet spin',*STLE, Tribology Transaction*, Vol.35, No. 2,pp.225-234.

[14] Greenwood, J.A. and Tripp, .J.H. 1970, 'The contact of two nominally flat rough surfaces', *Proc. Instn. Mech. Engrs. ,* Vol. 185, pp. 625-633.

[15] Han, D.C. 1979, *Statische und dynamische Eigenschaften von Gleitlagern bei hahen Umfangsgeschwindigkeoten und hei Verkantung*, Dissertaion, Universitat Karlsruhe.

[16] Hoshi, Mi 1984, 'Reducing Friction Losses in Automobile Engineers', *Tribology International*, Vol. 17, No. 4, pp 185-189.

[17] Ito, A., Yang, L. and Negishi, H. 1998, 'A Study on Cam Wear Mechanism With a Newly Delveoped Friction Measurement Apparatus', *SAE* Paper No. 982663.

[18] Johanson, K.L. 1985, *Contact Mechanics* (Cambridge University Press).

[19] Martin F A 1985, 'Friction in internal Combustion Engine Bearings'. In combustion Engines – Reduction of Friction and Wear. Paper C67/85, *IMechE* Conference Publications, pp 1-7.

[20] Monteil, Gallmann, A., Sioshansi, P. and Loges, P. and Loges, P. 1996, 'Contribution of Nuclear Physics to Engine Design: Application of Surface Layer Activation to Tappet Rotation Measurements', *SAE* 960711.

[21] Muller R 1966, 'The effect of Lubrication on Cam and Tappet Performance', *Motor Tech Z* , Vol 27 , Pt 2, pp 58-6, MIRA Translation, No 27/66

[22] Martin H M 1916, 'Lubrication of Gear Teeth', Engineering, London, 102, pp 199.

[23] Nemlekar, P.R. and Cheng, H.S. 1980, 'Traction in rough Elastrohydrodynamic contacts'.

[24] Parker, D.A., Adams, D.R., and Barrent, D. J.S. 'The Reduction of Friction in the Internal Combustion Engine', SAE Symposium, Paper No. 29.

[25] Pieprzak, J.M., Willermet, P.A. and Dailey, D.P. 1990, 'Experimental Evaluation of Tappet/Bore and Cam/Tappet Friction for a Direct Acting Bucket Tappet Valvetrain', *SAE* 902086.

[26] Pieprzak, J.M., Willermet, P.A. and Klassen, D. 1989, 'A Tappet Rotation Monitor Based on Light Reflectance-Development and Functional Testing', *SAE* 890722.

[27] Parker D A and Adams D R 1982, 'Friction Losses in the Reciprocating Internal Combustion Engine', in Tribology - Key to the Efficient Engine, Paper C5/82, *IMechE* Conference Publication, pp 31-39.

[28] Polak T A and Lette A 1987, 'When did you last change your Camshaft?' *Automobile Engineer,* Vol 12 , No 3, June/July 1987, pp6-8.

[29] Pinkus, O. and Sternlicht, B. 1961, *Theory of Hydrodynamic Lubrication* , McGraw-Hill Book Company.

[30] Riaz, Priest, 'Experimental and Theoretical Study of Instantaneous Engine Valve Train Friction', Proceedings of 2002 ASME/STLE Joint International Tribology Conference, Mexico

[31] Taylor, C.M. 1993, Engine Tribology, Tribology Series 26, Elsevier Science Publishers.

[32] Taylor C M 1991, 'Valve Train Lubrication Analysis', Proc of 17th Leeds – Lyon Symposium on Tribology in Vehicle Tribology, Elsevier, to be published

[33] Van Helden, A.K., Van der Meer, R.J., Van Staaden, J.J. and Van Gelderen, E. 1985, 'Dynamic Friction in Cam/Tappet Lubrication', *SAE* 850441.

[34] Willermet, P.A., Pieprzak, J.M. 1989, 'Some effects of lubricant composition and tappet rotation on Cam/Tappet friction', Transaction of ASME, *Journal of Tribology*, Vol. 111, pp.683-691.

[35] Willermet 1988, 'Tribological design -The automotive industry', Proceedings of the 15th Leeds-Lyon Symposium on Tribology held at Bodington Hall, The University of Leeds, U K

[36] Willermert, P.A., Pieprzak, and Dailey, D.P. 1990, 'Tappet rotation and friction reduction in a center pivot rocker arm contact', Transaction of ASME , *Journal of Tribology*, Vol. 112, pp.655-661.

[37] Yang, L, Ito, A, and Negishi, H. 1998, 'A Valve Train friction and Lubrication Analysis Model and Its Application in a Cam/tappet Wear Study', *SAE* 962030.

[38] Zhu, G. 1988, *A theoretical and experiment study of the tribology of the tribology of a cam and follower*, PhD thesis, Mechanical Engineering Department, Leeds University, UK.

[39] Zhu,G. C.M. Taylor, *'Tribological Analysis and Design of a Modern Automobile Cam and Follower'*, Engineering Research Series.

Annexure A

Matlab Code for Direct Acting Valve Train

```
function
[hmin,Omega,WL,Ve,hcen,Ttorque,Fc,v,a,Vs,R,avgOmega,totalpowerLos,powerLosYang,powe
rLosrough] = atiq1(w,mewLimit,no,Omega,O,l,l1)
```

Input Data

```
Rb=.017;
w = w*.10471;
t=(O .*2.77*10^-4)
k=35838;
springx=.00859;
m = .042;
MS = .073;
clr=.00003;
u1 = .28 ;     %poison ratio for cam
u2 = .3 ;      % poison ratio for follower
E1=172* 10^9;  % youngs modulus of cam
E2 = 204 * 10^9;   % youngs modulus of follower
WC= .014 ;
pie  =3.14;
alpha = .15 * 10^-7 ;
mewa = .2; % asperty slding coeff of fric
Taw0 = 8*10^6;       % Eyring stress
TawL = 6*10^6   ;    %  limiting Eyring Stress
Gamm = .008;
Lf= .026;
Rf=0  ;            % Follower rad ov curva
```

```
Df=.0320 ;       %m      Follower dia
Db= .0326;       %m        tapp bore di
alphad=0;     J = 1.6*10^-6;     %moment of inertia of follower   kgm2/s
mewb = .12;  % units check    %frict coeff of boundr lubri    che value
oa= .2*10^-6;
naBoa=.05;
d1=.14704*10^-40;
d2=.70373*10^2;
d3=-.12696*10^2;
d4=.74104*10^-21;
d5=.30813*10^2;
d6=-.36470*10^1;
d7=.88123*10^-4;
d8=.21523*10^1;
f1=.11755*10^-39;
f2=.67331*10^2;
f3=-.11699*10^2;
f4=.15827*10^-20;
f5=.29156*10^2;
f6=-.29786*10^1;
f7=.11201*10^-3;
f8=.19447*10^1;
H1=9;
H2=8;
H3=4;
St=0;
sqrtoaB=1*10^-3;
%%%%%%%%%%%%%%%%%%%%%%%%%%%%%%%%%%%%%%%%%%%%%%%%
```

Velocity Calculation

```
v =v_cal(t );
e = v./w;
```

```
a =a_cal(t,w );
```

Acceleration Calculation

```
function a = a_cal(t,w )
l =l./1000;
O1=O.*0.0174532925;
lenl= size(l,2);
a=[0 0 0 0  ];
for i=2:lenl-3

    tempa= ((2*l(i)-5*l(i+1)+4*l(i+2)-l(i+3))/((O1(i+1)-O1(i))*(O1(i+3)-O1(i+2))))*w^2;

     a=[a tempa];

end;
end



%%%%%%%%%%%%%%%%%%%%%%%%%%%%%%%%%%%%%%%%%%%%%%%%%%%%%%%%%%%%%%%%%%%%%%%%%%%%%%%%%%%%%%%%%%%%%%%%%%%%
%%%
```

Equvalent Elastic Modulus

```
E = .5 * (((1-u1^2)/E1) + ((1-u2^2)/E2));
Eequ =1/ E;
%%%%%%%%%%%%%%%%%%%%%%%%%%%%%%%%%%%%%%%%%%%%%%%%%%%%%%%%%%%%%%%%%%%%%%%%%%%%%%%%%%%%%%%%%%%%%%%%%%%%
%%%
```

Radius of Curvature

```
R = R_cal(Rb,a,w);
function R = R_cal(Rb,a,w )
l =l./1000;
lenl= size(l,2);
```

```
R=[ 0.017 0.017 ];
for i=2:1:lenl-1
   tempR=  Rb + l(i-1) + ( a(i)./w^2);
   R=[R tempR];
end
end

Requ=abs(R);

%%%%%%%%%%%%%%%%%%%%%%%%%%%%%%%%%%%%%%%%%%%%%%%%%%%%%%%%%%%%%%%%%%%%%%%%
%
```

Contact Load

```
WL =WL_cal(springx,l,MS,m,a,clr,l1,k );
 function WL =WL_cal(springx,l,MS,m,a,clr,l1,k )

WL= (k.*(l + springx) + (MS + (1/3).*m).*a).*(l1>clr)+65;

end

%%%%%%%%%%%%%%%%%%%%%%%%%%%%%%%%%%%%%%%%%%%%%%%%%%%%%%%%%%%%%%%%%%%%%%%%
```

Calculation of Entraining Velocity:

```
for qqq=1:360
Vc(qqq)=(R(qqq))*w;
Vf(qqq)= ((a(qqq)/w));
Ve(qqq)=(.5*(((Vf(qqq)))+(Vc(qqq))));
```

Calculation of Hertzian Contact Pressure:

```
b(qqq)= sqrt((8*abs(WL(qqq))* abs(Requ(qqq)))/(pi* WC*Eequ)) ;
Pmax(qqq)= ( 2*WL(qqq)) / (pi *b(qqq) *WC );
```

```
%%%%%%%%%%%%%%%%%%%%%%%%%%%%%%%%%%%%%%%%%%%%%%%%
%%%%%%%%%%%%%%
```

Calculation of Minimum Film Thickness

```
U1(qqq) = abs(((Ve(qqq)) )* no)/ (Eequ * abs(Requ(qqq))) ;%equ const and requ
G(qqq) = (alpha * Eequ);
Wnp(qqq) = abs(WL(qqq)/(Eequ * abs( Requ(qqq))));
hmin(qqq) =hmin_cal(Requ(qqq),U1(qqq), G(qqq) ,Wnp(qqq));
hcen(qqq) =hcen_cal(Requ(qqq),U1(qqq), G(qqq) ,Wnp(qqq));

%%%%%%%%%%%%%%%%%%%%%%%%%%%%%%%%%%%%%%%%%%%%%%%%
%%%%%%%%%%%%%%
```

Calculation of Sliding Velocity

```
z(qqq) =z_cal( b(qqq) );
z1(qqq)=exp(z(qqq)*alpha.* Pmax(qqq));
P(qqq)=Pmax(qqq)*z(qqq);
n(qqq) = no* exp(alpha* P(qqq));
Vs(qqq) =(Vc(qqq)) - (a(qqq)/w);

%%%%%%%%%%%%%%%%%%%%%%%%%%%%%%%%%%%%%%%%%%%%
```

Calculation of Friction and friction torque

```
F1(qqq) =F1_cal(z1(qqq),Vs(qqq),no,hcen(qqq),l1(qqq),clr);

Flimit(qqq) = (mewLimit.*WL(qqq));
if w <1100*.10471;
  if F1(qqq)  < Flimit(qqq)
    F1(qqq)=Flimit(qqq);
  end
end
F2(qqq) = min(F1(qqq),Flimit(qqq));
cf(qqq) =((F2(qqq) *WC)/WL(qqq) ).*(l1(qqq)>clr)+ 0;
```

Ttorque(qqq) =Ttorque_cal(e(qqq),WL(qqq),F2(qqq) ,WC,Rb,l(qqq));

%%

U111(qqq) = sqrt(((Df*Omega(qqq))/2).^2 + (v(qqq).^2));

%%

h(qqq) = hcen(qqq);
H(qqq)=h(qqq)./oa;
Fri1(qqq) =Fri1_cal(d1,d2,d3,d4 ,d5,d6,d7,d8,H(qqq),H1,H2,H3);
Fri2(qqq) =Fri2_cal(f1,f2,f3,f4 ,f5,f6,f7,f8,H(qqq),H1,H2,H3);

%%

<u>Calculation of Asperity Contact Load and Friction</u>

A(qqq)=2*b(qqq)*WC;
Aa(qqq)=(3.14^2*(naBoa)^2).*(A(qqq).*Fri1(qqq).*(h(qqq)./oa));
Wa(qqq) =((8*sqrt(2))/15)*3.14*(naBoa)^2*Eequ*sqrtoaB.*(A(qqq).*Fri2(qqq).*(h(qqq)./oa));
Cf =(Db-Df)/2;
Fc(qqq) =Fc_cal(mewa,Wa(qqq),Aa(qqq),A(qqq),F2(qqq));

%%
%

<u>Calculation of Reaction Forces and Eccentricities</u>

d(qqq)=sqrt(e(qqq).^2 + St^2);
Wb2(qqq)=(d(qqq)./Lf).*WL(qqq);
Wb1(qqq)=(Wb2(qqq)-Fc(qqq));
fun1e(qqq) =fun1e_cal(Cf,abs(Wb1(qqq)),Lf,U111(qqq),n(qqq));
fun2e(qqq) =fun2e_cal(Cf,abs(Wb2(qqq)),Lf,U111(qqq),n(qqq));
ecc1(qqq)=fun1e(qqq)*Cf;

```
ecc2(qqq)=fun2e(qqq)*Cf;

%%%%%%%%%%%%%%%%%%%%%%%%%%%%%%%%%%%%%%%%%%%%%%
%%%
nab(qqq)=n(qqq);
deltaFt(qqq) =deltaFt_cal(Taw0,TawL,Gamm,Pmax(qqq)
,Vs(qqq),hcen(qqq),n(qqq),mewa,Aa(qqq),A(qqq),Wa(qqq));
```

<u>Calculation of DeltaFt</u>

```
function deltaFt =deltaFt_cal(Taw0,TawL,Gamm,Pmax,Vs,hcen,n,mewa,Aa,A,Wa)
Taw= n.* (Vs./hcen);
 Taw = Taw.*(Taw<=Taw0);
Taw2 = Taw0 + (Gamm.*Pmax);
Taw = Taw + Taw2.*(Taw2>Taw0 & Taw2<=TawL);
Taw= Taw + TawL.*(Taw==0);
deltaFt = (mewa.*(Wa./A)) + ((1 - (Aa./A)).*Taw);
end

%%%%%%%%%%%%%%%%%%%%%%%%%%%%%%%%%%%%%%%%%%%%%%
%%
%%%%%%%%%%%%%%%%%%%%%%%%%%%%%%%%%%%%%%%%%%%%%%
%%%
```

<u>Calculation of Friction at Tappet Bore Contact</u>

```
 taw11(qqq) = (atan((2*(ecc1(qqq)+ecc2(qqq)))./Lf));
   Cb1(qqq) = Cf - ecc1(qqq) - ((Lf*tan(taw11(qqq)))./4);
   Cb2(qqq) = Cf - ecc2(qqq) - ((Lf*tan(taw11(qqq)))./4);
   oafb =oa  ;% ??????????????? is it oafb is com rough height btw foll bore ,other oa btw cam
foll
   lamda1(qqq) = Cb1(qqq)/oafb;
   k11(qqq)= lamda1(qqq)./3;
   lamda2(qqq) = Cb2(qqq)/oafb;
```

```
    k12(qqq)= lamda2(qqq)./3;
    vf(qqq)=v(qqq);
    if(lamda1(qqq)>3)
        Ff1(qqq) = ((((pie*nab(qqq)*Df*Lf).*U111(qqq)).*vf(qqq))./(2*Cf.*U111(qqq).*sqrt(1-
fun1e(qqq).^2)));
    elseif(lamda1(qqq)>=0 && lamda1(qqq)<=3)
        Ff1(qqq) = (((((((1-
k11(qqq))*mewb).*Wb1(qqq)).*vf(qqq))+(((k11(qqq)*3.14*Lf*Df*nab(qqq)).*vf(qqq).*U111(
qqq))./(2*Cf.*sqrt(1-(fun1e(qqq)).^2)))))./U111(qqq)));
    elseif(lamda1(qqq)<0)
        Ff1(qqq) = ((mewb.*Wb1(qqq).*vf(qqq)./U111(qqq)));
    end

        if(lamda2(qqq)>3)
        Ff2(qqq) = ((((pie*nab(qqq)*Df*Lf).*U111(qqq)).*vf(qqq))./(2*Cf.*U111(qqq).*sqrt(1-
fun2e(qqq).^2)));
    elseif(lamda2(qqq)>=0 && lamda2(qqq)<=3)
        Ff2(qqq) = (((((((1-
k12(qqq))*mewb).*Wb2(qqq)).*vf(qqq))+(((k12(qqq)*3.14*Lf*Df*nab(qqq)).*vf(qqq).*U111(
qqq))./(2*Cf.*sqrt(1-(fun2e(qqq)).^2)))))./U111(qqq)));
    elseif(lamda2(qqq)<0)
        Ff2(qqq) = ((mewb.*Wb2(qqq).*vf(qqq)./U111(qqq)));
        End
%%%%%%%%%%%%%%%%%%%%%%%%%%%%%%%%%%%%%%%%%%%%%%%%%%%%%%
%%%%%%%%%%%%%%%%%%%
```

<u>Calculation of Tappet Rotation</u>

```
J = 1.9*10^-6;     %moment of inertia of follower   kgm2/s
Omega =0
 h=1
for qqq = 1: 2000
```

```
    d11=1


   Tfc=-3.18428390776730;
   Tfb =-10.3615798569449;
OmegaDot = ((Tfc - Tfb))./J


   Omega1 = Omega + (OmegaDot*(.0000001))
%    rr= (abs(((Omega-Omega1)/Omega1)))*100


if abs(((Omega-Omega1))/(Omega1))<.001
       Omega = Omega1;
     c=1
       break;
else
    Omega=Omega1
    h=h+1
    continue;
   h=h+1
end


end


%%%%%%%%%%%%%%%%%%%%%%%%%%%%%%%%%%%%%%%%%%%%%%%%%%%
%%%%%
Tc(qqq)= Fc(qqq)*.008./WC
Ff(qqq) = Ff1(qqq) + Ff2(qqq);
Tfb(qqq) =(((Omega(qqq))*(Df^2)*(Ff1(qqq)+Ff2(qqq)))/(4*v(qqq)));
Tj(qqq)=.0035*WL(qqq)
Omega(qqq+1) = omega_cal( (Tfb(qqq)),Tc(qqq),Tj(qqq) );
end
avgOmega=sum(sum(Omega))./360
```

```
hmin(180:210)=hpfilter(hmin(180:210),400);
hmin(180:210) = smooth(hmin(180:210),40);
%
%%%%%%%%%%%%%%%%%%%%%%%%%%%%%%%%%%%%%%%%%%%%%%%%%%%%%%%%%%%%%%%%%%%%%%%%%%%%%%%
%%%

%
%%%%%%%%%%%%%%%%%%%%%%%%%%%%%%%%%%%%%%%%%%%%%%%%%%%%%%%%%%%%%%%%%%%%%%%%%%%%%%%
%%%%%5
```

Power Loss Calculation

```
powerLosYang =  (((((sum(F2.*(R))))).*w)/(360));
powerLosrough = (((((sum(Fc.*(R))))).*w)/(360));
dia =.007; %m
leng = .035;%m
clea = .00002;%m
Fv = (n.*v.*3.14*dia*leng)./(clea);
Tf = (Ff + Fv ).*(Rb+l);
Tc = Fc.*(Rb+l);
Tfric = Tf+ Tc ;
totalpowerLos =w.*((sum(sum(Tfric)))./(360));
end
```

Parametric Study

Velocity- Acceleration

```
w =400;
mewLimit =.12;
no=(9.72*10^-6)*1000;
Omega =200*.10471.*ones(1,360);
[hmin4,Omega4,WL4,Ve4,hcen4,Ttorque4,Fc4,v,a,Vs,R,avgOmega,totalpowerLos4,powerLosY
ang4,powerLosrough4] = atiq(w,mewLimit,no,Omega,O,l,l1);
% totalpowerLos4
% powerLosYang4
```

```
% powerLosrough4
f = figure(60);
plot(O,v,'k');

xlabel('Degrees');
ylabel('velocity (m/s)');
title('Tappet Velocity');
print(f,'-djpeg', 'C:\Users\ars\Desktop\result\v.fig');
f = figure(61);
 a=hpfilter(a,3);
 a(180:210)=hpfilter(a(180:210),400);
 a(180:210) = smooth(a(180:210),40);
plot(O,a,'k');
xlabel('Degrees');
ylabel('Accleration(m/s^2)');
title('Tappet Accleration');
print(f,'-djpeg', 'C:\Users\ars\Desktop\result\a.fig');
 Vs=hpfilter(Vs);
 f = figure(62);

plot(O,Vs,'k');
xlabel('Degrees');
ylabel('Sliding Velocity');
title('Sliding Velocity');
print(f,'-djpeg', 'C:\Users\ars\Desktop\result\Vs.fig');

f = figure(63);
 R(180:210)=hpfilter(R(180:210),400);
 R(180:210) = smooth(R(180:210),40);
plot(O,R,'k');
xlabel('Degrees');
```

```
ylabel('Radius of Curvature (m)');
title('Radius of Curvature');
print(f,'-djpeg', 'C:\Users\ars\Desktop\result\R.fig');
```

Effect of Temperature on Valve Train Performance:

```
%Temperature all
Limiting Coefficient of friction = .12
%low temp 40 c
w =400;
mewLimit =.12;
no=(39*10^-6)*1000;
Omega =200*.10471.*ones(1,130);
[hmin1,Omega1,WL1,Ve1,hcen1,Ttorque1,Fc1,v,a,Vs,R,avgOmega,totalpowerLos1,powerLosY
ang1,powerLosrough1] = atiq(w,mewLimit,no,Omega,O,l,l1);
totalpowerLos1
powerLosYang1
powerLosrough1
% temp 60 c
w =400;
mewLimit =.12;
no=(21.49*10^-6)*1000;
Omega =200*.10471.*ones(1,130);
[hmin2,Omega2,WL2,Ve2,hcen2,Ttorque2,Fc2,v,a,Vs,R,avgOmega,totalpowerLos2,powerLosY
ang2,powerLosrough2] = atiq(w,mewLimit,no,Omega,O,l,l1);
totalpowerLos2
temp 80
w =400;
mewLimit =.12;
no=(13.26*10^-6)*1000;
Omega =200*.10471.*ones(1,130);
```

```
[hmin3,Omega3,WL3,Ve3,hcen3,Ttorque3,Fc3,v,a,Vs,R,avgOmega,totalpowerLos3,powerLosY
ang3,powerLosrough3] = atiq(w,mewLimit,no,Omega,O,l,l1);
totalpowerLos3
temp 95
w =400;
mewLimit =.12;
no=(9.72*10^-6)*1000;
Omega =200*.10471.*ones(1,130);
[hmin4,Omega4,WL4,Ve4,hcen4,Ttorque4,Fc4,v,a,Vs,R,avgOmega,totalpowerLos4,powerLosY
ang4,powerLosrough4] = atiq(w,mewLimit,no,Omega,O,l,l1);
% totalpowerLos4
f = figure(2);

plot(O,hmin1,'r');hold on;
plot(O,hmin2,'g');hold on
plot(O,hmin3,'b');hold on
plot(O,hmin4,'k');hold off
xlabel('Degrees');
ylabel('Minimum Film Thickness(m)');
title('At 400 RPM');
legend('40 C','60 C','80 C','95 C');
print(f,'-djpeg', 'C:\Users\ars\Desktop\result\hminTemlowv.fig');
%
f = figure(3);
plot(O2,Omega1,'r');hold on;
plot(O2,Omega2,'g');hold on
plot(O2,Omega3,'b');hold on
plot(O2,Omega4,'k');hold off
xlabel('Degrees');
ylabel('Tappet Roattion(RPM)');
title('At 400 RPM');
```

```
legend('40 C','60 C','80 C','95 C');
print(f,'-djpeg', 'C:\Users\ars\Desktop\result\OmegaTempRotlowv.fig');
f = figure(4);

plot(O,Fc1,'r');hold on;
plot(O,Fc2,'g');hold on
plot(O,Fc3,'b');hold on
plot(O,Fc4,'k');hold off
xlabel('Degrees');
ylabel('Cam Tappet friction(N)');
title('At 400 RPM');
legend('40 C','60 C','80 C','95 C');
print(f,'-djpeg', 'C:\Users\ars\Desktop\result\FcTemlowv.fig');
f = figure(5);
plot(O,WL1,'r');hold on;
plot(O,WL2,'g');hold on
plot(O,WL3,'b');hold on
plot(O,WL4,'k');hold off
xlabel('Degrees');
ylabel('Vertical Loading(N)');
title('At 400 RPM');
legend('40 C','60 C','80 C','95 C');
print(f,'-djpeg', 'C:\Users\ars\Desktop\result\WLTemlowv.fig');
%low temp 40, high speed
w =1000;
mewLimit =.12;
no=(39*10^-6)*1000;
Omega =200*.10471.*ones(1,130);
[hmin5,Omega5,WL5,Ve5,hcen5,Ttorque5,Fc5,v,a,Vs,R,avgOmega,totalpowerLos5,powerLosY
ang5,powerLosrough5] = atiq(w,mewLimit,no,Omega,O,l,l1);
```

```
temp 60 c
w =1000;
mewLimit =.12;
no=(21.49*10^-6)*1000;
Omega =200*.10471.*ones(1,130);
[hmin6,Omega6,WL6,Ve6,hcen6,Ttorque6,Fc6,v,a,Vs,R,avgOmega,totalpowerLos6,powerLosY
ang6,powerLosrough6] = atiq(w,mewLimit,no,Omega,O,l,l1);
temp 80
w =1000;
mewLimit =.12;
no=(13.26*10^-6)*1000;
Omega =200*.10471.*ones(1,130);
[hmin7,Omega7,WL7,Ve7,hcen7,Ttorque7,Fc7,v,a,Vs,R,avgOmega,totalpowerLos7,powerLosY
ang7,powerLosrough7] = atiq(w,mewLimit,no,Omega,O,l,l1);
% temp 95
w =1000;
mewLimit =.12;
no=(9.72*10^-6)*1000;
Omega =200*.10471.*ones(1,130);
[hmin8,Omega8,WL8,Ve8,hcen8,Ttorque8,Fc8,v,a,Vs,R,avgOmega,totalpowerLos8,powerLosY
ang8,powerLosrough8] = atiq(w,mewLimit,no,Omega,O,l,l1);
totalpowerLos5
totalpowerLos6
totalpowerLos7
totalpowerLos8

f = figure(6);
plot(O,hmin5,'r');hold on;
plot(O,hmin6,'g');hold on
plot(O,hmin7,'b');hold on
plot(O,hmin8,'k');hold off
```

```
xlabel('Degrees');
ylabel('Minimum Film Thickness(m)');
title('At 1000 RPM');
legend('40 C','60 C','80 C','95 C');
print(f,'-djpeg', 'C:\Users\ars\Desktop\result\hmintemhighv.jpg');

f = figure(7);
plot(O2,Omega5,'r');hold on;
plot(O2,Omega6,'g');hold on
plot(O2,Omega7,'b');hold on
plot(O2,Omega8,'k');hold off
xlabel('Degrees');
ylabel('Tappet Roattion(RPM)');
title('At 1000 RPM');
legend('95 C','80 C','60 C','40 C');
print(f,'-djpeg', 'C:\Users\ars\Desktop\result\Omegatemrothighv.jpg');

f = figure(8);
plot(O,Fc5,'r');hold on;
plot(O,Fc6,'g');hold on
plot(O,Fc7,'b');hold on
plot(O,Fc8,'k');hold off
xlabel('Degrees');
ylabel('Cam Tappet friction(N)');
title('At 1000 RPM');
legend('95 C','80 C','60 C','40 C');
print(f,'-djpeg', 'C:\Users\ars\Desktop\result\Fctemhighv.jpg');

f = figure(9);
plot(O,WL5,'r');hold on;
plot(O,WL6,'g');hold on
```

```
plot(O,WL7,'b');hold on
plot(O,WL8,'k');hold off
xlabel('Degrees');
ylabel('Vertical loading(N)');
title('At 1000 RPM');
legend('40 C','60 C','80 C','95 C');
print(f,'-djpeg', 'C:\Users\ars\Desktop\result\WLtemhighv.jpg');
%%%%%%%%%%%%%%%%%%%%%%%%%%%%%%%%%%%%%%%%%%%%
%%
```

Effect of Engine Speed on Valve Train Performance:

```
w =400;
mewLimit =.12;
no=(39*10^-6)*1000;
Omega =200*.10471.*ones(1,130);
[hmin11,Omega11,WL11,Ve11,hcen11,Ttorque11,Fc11,v,a,Vs,R,avgOmega,totalpowerLos11,p
owerLosYang11,powerLosrough11] = atiq(w,mewLimit,no,Omega,O,l,l1);


temp 95
w =400;
mewLimit =.12;
no=(9.72*10^-6)*1000;
Omega =200*.10471.*ones(1,130);
[hmin22,Omega22,WL22,Ve22,hcen22,Ttorque22,Fc22,v,a,Vs,R,avgOmega,totalpowerLos22,p
owerLosYang22,powerLosrough22] = atiq(w,mewLimit,no,Omega,O,l,l1);


low temp 40, high speed
w =1000;
mewLimit =.12;
```

```
no=(39*10^-6)*1000;
Omega =200*.10471.*ones(1,130);
[hmin33,Omega33,WL33,Ve33,hcen33,Ttorque33,Fc33,v,a,Vs,R,avgOmega,totalpowerLos33,p
owerLosYang33,powerLosrough33] = atiq(w,mewLimit,no,Omega,O,l,l1);

temp 95
w =1000;
mewLimit =.12;
no=(9.72*10^-6)*1000;
Omega =200*.10471.*ones(1,130);
[hmin44,Omega44,WL44,Ve44,hcen44,Ttorque44,Fc44,v,a,Vs,R,avgOmega,totalpowerLos44,p
owerLosYang44,powerLosrough44] = atiq(w,mewLimit,no,Omega,O,l,l1);
totalpowerLos11
totalpowerLos22
totalpowerLos33
totalpowerLos44


f = figure(10);
plot(O,hmin11,'r');hold on;
plot(O,hmin33,'k');hold off
xlabel('Degrees');
ylabel('Minimum Film Thickness(m)');
title('Engine Speed');
legend('400 RPM AT 40 C','1000 RPM AT 40 C');
print(f,'-djpeg', 'C:\Users\ars\Desktop\result\hminspelowtemp.jpg');
f=figure(1133)
plot(O,Ve11,'r');hold on;
plot(O,Ve33,'k');hold off
xlabel('Degrees');
ylabel('Entraining Velocity');
```

```
title('Engine Speed');
legend('400 RPM AT 40 C','1000 RPM AT 40 C');
print(f,'-djpeg', 'C:\Users\ars\Desktop\result\Vespelowtemp.jpg');

f = figure(11);
plot(O2,Omega11,'r');hold on;
plot(O2,Omega33,'k');hold off
xlabel('Degrees');
ylabel('Tappet Roattion(RPM)');
title('Engine Speed');
legend('400 RPM AT 40 C','1000 RPM AT 40 C');
print(f,'-djpeg', 'C:\Users\ars\Desktop\result\Omegaspelowtemp.jpg');


f = figure(12);
plot(O,Fc11,'r');hold on;
plot(O,Fc33,'k');hold off
xlabel('Degrees');
ylabel('Cam Tappet friction(N)');
title('Engine Speed');
legend('400 RPM AT 40 C','1000 RPM AT 40 C');
print(f,'-djpeg', 'C:\Users\ars\Desktop\result\Fcspelowtemp.jpg');

f = figure(13);
plot(O,WL11,'r');hold on;
plot(O,WL33,'k');hold off
xlabel('Degrees');
ylabel('Vertical loading(N)');
title('Engine Speed');
legend('400 RPM AT 40 C','1000 RPM AT 40 C');
print(f,'-djpeg', 'C:\Users\ars\Desktop\result\WLspelowtemp.jpg');
```

```
f = figure(14);
plot(O,hmin22,'r');hold on;
plot(O,hmin44,'k');hold off
xlabel('Degrees');
ylabel('Minimum Film Thickness(m)');
title('Engine Speed');
legend('400 RPM AT 95 C','1000 RPM AT 95 C');

print(f,'-djpeg', 'C:\Users\ars\Desktop\result\hminspehigtemp.jpg');

f = figure(15);
plot(O2,Omega22,'r');hold on;
plot(O2,Omega44,'k');hold off
xlabel('Degrees');
ylabel('Tappet Roattion(RPM)');
title('Engine Speed');
legend('400 RPM AT 95 C','1000 RPM AT 95 C');

print(f,'-djpeg', 'C:\Users\ars\Desktop\result\Omegaspehigtemp.jpg');

f = figure(16);
plot(O,Fc22,'r');hold on;
plot(O,Fc44,'k');hold off
xlabel('Degrees');
ylabel('Cam Tappet friction(N)');
title('Engine Speed');
legend('400 RPM AT 95 C','1000 RPM AT 95 C');

print(f,'-djpeg', 'C:\Users\ars\Desktop\result\Fcspehigtemp.jpg');

f = figure(17);
```

```
plot(O,WL22,'r');hold on;
plot(O,WL44,'k');hold off
xlabel('Degrees');
ylabel('Vertical loading(N)');
title('Engine Speed');
legend('400 RPM AT 95 C','1000 RPM AT 95 C');
print(f,'-djpeg', 'C:\Users\ars\Desktop\result\WLspehigtemp.jpg');
plot(O,Ve22,'r');hold on;
plot(O,Ve44,'k');hold off
xlabel('Degrees');
ylabel('Entraining Velocity');
title('Engine Speed');
legend('400 RPM AT 40 C','1000 RPM AT 40 C');
print(f,'-djpeg', 'C:\Users\ars\Desktop\result\Vespehigtemp.jpg');
%%%%%%%%%%%%%%%%%%%%%%%%%%%%%%%%%%%%%%%%%%%%
%%%%%%%%%%%%%%%%%%%5555
```

Effect of Friction Modifier on Valve Train Performance:

```
w =400;
mewLimit =.08;
no=(9.72*10^-6)*1000;
Omega =200*.10471.*ones(1,360);
[hmin55,Omega55,WL55,Ve55,hcen55,Ttorque55,Fc55,v,a,Vs,R,avgOmega,totalpowerLos55,p
owerLosYang55,powerLosrough55] = atiq(w,mewLimit,no,Omega,O,l,l1);

temp 95
w =400;
mewLimit =.12;
no=(9.72*10^-6)*1000;
Omega =200*.10471.*ones(1,360);
[hmin66,Omega66,WL66,Ve66,hcen66,Ttorque66,Fc66,v,a,Vs,R,avgOmega,totalpowerLos66,p
owerLosYang66,powerLosrough66] = atiq(w,mewLimit,no,Omega,O,l,l1);
```

```
totalpowerLos55
totalpowerLos66
hmin55(180:210)=hpfilter(hmin55(180:210),400);
 hmin55(180:210) = smooth(hmin55(180:210),40);
  hmin66(180:210)=hpfilter(hmin66(180:210),400);
 hmin66(180:210) = smooth(hmin66(180:210),40);

f = figure(18);
plot(O,hmin55,'r');hold on;
plot(O,hmin66,'k');hold off

xlabel('Degrees');
ylabel('Minimum Film Thickness(m)');
title('Friction Modifier');
legend('400 RPM AT µlimit= .08','400 RPM AT µlimit=.12');



print(f,'-djpeg', 'C:\Users\ars\Desktop\result\hminmew812spelow.jpg');

f = figure(19);
plot(O2,Omega55,'r');hold on;
plot(O2,Omega66,'k');hold off
xlabel('Degrees');
ylabel('Tappet Roattion(RPM)');
title('Friction Modifier');
legend('400 RPM AT µlimit= .08','400 RPM AT µlimit=.12');

print(f,'-djpeg', 'C:\Users\ars\Desktop\result\Omegamew812spelow.jpg');

f = figure(20);
plot(O,Fc55,'r');hold on;
```

```
plot(O,Fc66,'k');hold off
xlabel('Degrees');
ylabel('Cam Tappet friction(N)');
title('Friction Modifier');
legend('400 RPM AT µlimit= .08','400 RPM AT µlimit=.12');

print(f,'-djpeg', 'C:\Users\ars\Desktop\result\Fcmew812spelow.jpg');

f = figure(21);
plot(O,WL55,'r');hold on;
plot(O,WL66,'k');hold off
xlabel('Degrees');
ylabel('Vertical loading(N)');
title('Friction Modifier');
legend('400 RPM AT µlimit= .08','400 RPM AT µlimit=.12');
print(f,'-djpeg', 'C:\Users\ars\Desktop\result\WLmew812spelow.jpg');
%low temp 40, high speed
w =1000;
mewLimit =.08;
no=(9.72*10^-6)*1000;
Omega =200*.10471.*ones(1,360);
[hmin77,Omega77,WL77,Ve77,hcen77,Ttorque77,Fc77,v,a,Vs,R,avgOmega,totalpowerLos77,p
owerLosYang77,powerLosrough77] = atiq(w,mewLimit,no,Omega,O,l,l1);

% temp 95
w =1000;
mewLimit =.12;
no=(9.72*10^-6)*1000;
Omega =200*.10471.*ones(1,360);
[hmin88,Omega88,WL88,Ve88,hcen88,Ttorque88,Fc88,v,a,Vs,R,avgOmega,totalpowerLos88,p
owerLosYang88,powerLosrough88] = atiq(w,mewLimit,no,Omega,O,l,l1);
```

```
totalpowerLos77
totalpowerLos88
f = figure(22);
plot(O,hmin77,'r');hold on;
plot(O,hmin88,'k');hold off
xlabel('Degrees');
ylabel('Minimum Film Thickness(m)');
title('Friction Modifier');
legend('1000 RPM AT µlimit=.08','1000 RPM AT µlimit=.12');
print(f,'-djpeg', 'C:\Users\ars\Desktop\result\hminmew812spehgh.jpg');

f = figure(23);
plot(O2,Omega77,'r');hold on;
plot(O2,Omega88,'k');hold off
xlabel('Degrees');
ylabel('Tappet Roattion(RPM)');
title('Friction Modifier');
legend('1000 RPM AT µlimit= .08','1000 RPM AT µlimit=.12');

print(f,'-djpeg', 'C:\Users\ars\Desktop\result\Omegamew812spehgh.jpg');

f = figure(24);
plot(O,Fc77,'r');hold on;
plot(O,Fc88,'k');hold off
xlabel('Degrees');
ylabel('Cam Tappet friction(N)');
title('Friction Modifier');
legend('1000 RPM AT µlimit= .08','1000 RPM AT µlimit=.12');
print(f,'-djpeg', 'C:\Users\ars\Desktop\result\Fcmew812spehgh.jpg');

f = figure(25);
```

```
plot(O,WL77,'r');hold on;
plot(O,WL88,'k');hold off
xlabel('Degrees');
ylabel('Vertical loading(N)');
title('Friction Modifier');
legend('1000 RPM AT µlimit= .08','1000 RPM AT µlimit=.12');
print(f,'-djpeg', 'C:\Users\ars\Desktop\result\WLmew812spehgh.jpg')

%%%%%%%%%%%%%%%%%%%%%%%%%%%%%%%%%%%%%%%%%%%
%%%%%%%%%%%%%%%%
```

Effect of Surface Roughness on Valve Train Performance:

```
w =400;
mewLimit =.12;
no=(39*10^-6)*1000;
[hmin9,WL9,Ve9,hcen9,Ttorque9,cf9,F29,powerLosYang9] = yang_cal(w,mewLimit,no,O,l,l1);
temp 95
w =400;
mewLimit =.12;
no=(39*10^-6)*1000;
[hmin10,WL10,Ve10,hcen10,Ttorque10,cf10,Fc10,powerLosrough10] =
yangroughness_cal(w,mewLimit,no,O,l,l1)

f = figure(26)
plot(O,hmin9,'r');hold on;
plot(O,hmin10,'k');hold off
xlabel('Degrees');
ylabel('Minimum Film Thickness(m)');
title('Surface Roughness');
legend('400 RPM without Surface Roughness,40 C ','400 RPM with Surface Roughness,40 C');
print(f,'-djpeg', 'C:\Users\ars\Desktop\result\hminroug400temlow.jpg');
```

```
f = figure(27);
plot(O,F29,'r');hold on;
plot(O,Fc10,'k');hold off
xlabel('Degrees');
ylabel('Cam Tappet friction(N)');
title('Surface Roughness');
legend('400 RPM without Surface Roughness,40 C ','400 RPM with Surface Roughness,40 C');
print(f,'-djpeg', 'C:\Users\ars\Desktop\result\Fcroug400temlow..jpg');

f = figure(28);
plot(O,WL9,'r');hold on;
plot(O,WL10,'k');hold off
xlabel('Degrees');
ylabel('Vertical loading(N)');
title('Surface Roughness');
legend('400 RPM without Surface Roughness,40 C ','400 RPM with Surface Roughness,40 C');
print(f,'-djpeg', 'C:\Users\ars\Desktop\result\WLroug400temlow..jpg');
low temp 40, high speed
w =1000;
mewLimit =.12;
no=(39*10^-6)*1000;
[hmin99,WL99,Ve99,hcen99,Ttorque99,cf99,F299,powerLosYang99] =
yang_cal(w,mewLimit,no,O,l,l1);

temp 40
w =1000;
mewLimit =.12;
no=(39*10^-6)*1000;
[hmin1010,WL1010,Ve1010,hcen1010,Ttorque1010,cf1010,Fc1010,powerLosrough1010] =
yangroughness_cal(w,mewLimit,no,O,l,l1)
```

```
f = figure(29);
plot(O,hmin99,'r');hold on;
plot(O,hmin1010,'k');hold off
xlabel('Degrees');
ylabel('Minimum Film Thickness(m)');
title('Surface Roughness');
legend('1000 RPM without Surface Roughness,40 C ','1000 RPM with Surface Roughness,40
C');
print(f,'-djpeg', 'C:\Users\ars\Desktop\result\hminroug1000temlow..jpg');


f = figure(30);
plot(O,F299,'r');hold on;
plot(O,Fc1010,'k');hold off
xlabel('Degrees');
ylabel('Cam Tappet friction(N)');
title('Surface Roughness');
legend('1000 RPM without Surface Roughness,40 C ','1000 RPM with Surface Roughness,40
C');
print(f,'-djpeg', 'C:\Users\ars\Desktop\result\Fcroug1000temlow.jpg');

f = figure(31);
plot(O,WL99,'r');hold on;
plot(O,WL1010,'k');hold off
xlabel('Degrees');
ylabel('Vertical loading(N)');
title('Surface Roughness');
legend('1000 RPM without Surface Roughness,40 C ','1000 RPM with Surface Roughness,40
C');
print(f,'-djpeg', 'C:\Users\ars\Desktop\result\WLroug1000temlow.jpg')
```

```
f = figure(36);
plot(O,F214,'r');hold on;
plot(O,Fc24,'k');hold off
xlabel('Degrees');
ylabel('Cam Tappet friction(N)');
w =400;
mewLimit =.12;
no=(9.72*10^-6)*1000;
[hmin13,WL13,Ve13,hcen13,Ttorque13,cf13,F213,powerLosYang13] =
yang_cal(w,mewLimit,no,O,l,l1);
temp 95
w =400;
mewLimit =.12;
no=(9.7*10^-6)*1000;
[hmin23,WL23, Ve23,hcen23,Ttorque23,cf23,Fc23,powerLosrough23] =
yangroughness_cal(w,mewLimit,no,O,l,l1)

f = figure(32);
plot(O,hmin13,'r');hold on;
plot(O,hmin23,'k');hold off
xlabel('Degrees');
ylabel('Minimum Film Thickness(m)');
title('Surface Roughness');
legend('400 RPM without Surface Roughness,95 C ','400 RPM with Surface Roughness,95 C');
print(f,'-djpeg', 'C:\Users\ars\Desktop\result\hminroug400temhgh.jpg');

f = figure(33);
plot(O,F213,'r');hold on;
plot(O,Fc23,'k');hold off
xlabel('Degrees');
ylabel('Cam Tappet friction(N)');
```

```
title('Surface Roughness');
legend('400 RPM without Surface Roughness,95 C ','400 RPM with Surface Roughness,95 C');
print(f,'-djpeg', 'C:\Users\ars\Desktop\result\Fcroug400temhgh.jpg');

f = figure(34);
plot(O,WL13,'r');hold on;
plot(O,WL23,'k');hold off
xlabel('Degrees');
ylabel('Vertical loading(N)');
title('Surface Roughness');
legend('400 RPM without Surface Roughness,95 C ','400 RPM with Surface Roughness,95 C');
print(f,'-djpeg', 'C:\Users\ars\Desktop\result\WLroug400temhgh.jpg');
low temp 40, high speed
w =1000;
mewLimit =.12;
no=(9.7*10^-6)*1000;
[hmin14,WL14,Ve14,hcen14,Ttorque14,cf14,F214,powerLosYang14] =
yang_cal(w,mewLimit,no,O,l,l1);

temp 95
w =1000;
mewLimit =.12;
no=(9.7*10^-6)*1000;
[hmin24,WL24,Ve24,hcen24,Ttorque24,cf24,Fc24,powerLosrough24] =
yangroughness_cal(w,mewLimit,no,O,l,l1)
f = figure(35);
plot(O,hmin14,'r');hold on;
plot(O,hmin24,'k');hold off
xlabel('Degrees');
ylabel('Minimum Film Thickness(m)');
title('Surface Roughness');
```

```
legend('1000 RPM without Surface Roughness,95 C ','1000 RPM with Surface Roughness,95
C');
print(f,'-djpeg', 'C:\Users\ars\Desktop\result\hminroug1000temhgh.jpg');

title('Surface Roughness');
legend('1000 RPM without Surface Roughness,95 C ','1000 RPM with Surface Roughness,95
C');
print(f,'-djpeg', 'C:\Users\ars\Desktop\result\Fcroug1000temhgh.jpg');

f = figure(37);
plot(O,WL14,'r');hold on;
plot(O,WL24,'k');hold off
xlabel('Degrees');
ylabel('Vertical loading(N)');
title('Surface Roughness');
legend('1000 RPM without Surface Roughness,95 C ','1000 RPM with Surface Roughness,95
C');
print(f,'-djpeg', 'C:\Users\ars\Desktop\result\WLroug400temhgh.jpg')
f = figure(377);
plot(O,F214,'r');hold on;
plot(O,Fc24,'k');hold off
xlabel('Degrees');
ylabel('Cam Tappet friction(N)');
title('Surface Roughness');
legend('1000 RPM without Surface Roughness,95 C ','1000 RPM with Surface Roughness,95
C');
print(f,'-djpeg', 'C:\Users\ars\Desktop\result\Fcroug1000temhgh.jpg');

%%%%%%%%%%%%%%%%%%%%%%%%%%%%%%%%%%%%%%%%%%%%
%%%%%%%%%%%%%%%%%%%%%%%%
```

Effect of Tappet Rotation on Valve Train Performance:

```
w =400;
mewLimit =.12;
no=(39*10^-6)*1000;
Omega =200*.10471.*ones(1,130);
[hmin25,Omega25,WL25,Ve25,hcen25,Ttorque25,Fc25] = atiq(w,mewLimit,no,Omega,O,l,l1);

% temp 95
w =400;
mewLimit =.12;
no=(9.72*10^-6)*1000;
Omega =200*.10471.*ones(1,130);
[hmin26,Omega26,WL26,Ve26,hcen26,Ttorque26,Fc26] = atiq(w,mewLimit,no,Omega,O,l,l1);

% low temp 40, high speed
w =1000;
mewLimit =.12;
no=(39*10^-6)*1000;
Omega =200*.10471.*ones(1,130);
[hmin27,Omega27,WL27,Ve27,hcen27,Ttorque27,Fc27] = atiq(w,mewLimit,no,Omega,O,l,l1);

% temp 95
w =1000;
mewLimit =.12;
no=(9.72*10^-6)*1000;
Omega =200*.10471.*ones(1,130);
[hmin28,Omega28,WL28,Ve28,hcen28,Ttorque28,Fc28] = atiq(w,mewLimit,no,Omega,O,l,l1);
f = figure(38);

plot(O,hmin25,'r');hold on;
plot(O,hmin26,'g');hold on
```

```
plot(O,hmin27,'b');hold on;
plot(O,hmin28,'k');hold off
xlabel('Degrees');
ylabel('Minimum Film Thickness(m)');
title('Tappet Rotation');
legend('400 RPM at 40 C','400 RPM at 95 C','1000 RPM at 40 C','1000 RPM at 95 C');
print(f,'-djpeg', 'C:\Users\ars\Desktop\result\hmin2526.jpg');

f = figure(39);
plot(O2,Omega26,'r');hold on;
plot(O2,Omega25,'g');hold on
plot(O2,Omega28,'b');hold on;
plot(O2,Omega27,'k');hold off
xlabel('Degrees');
ylabel('Tappet Rotation(RPM)');
title('Tappet Rotation');
legend('400 RPM at 40 C','400 RPM at 95 C','1000 RPM at 40 C','1000 RPM at 95 C');
print(f,'-djpeg', 'C:\Users\ars\Desktop\result\Omega2526.jpg');

f = figure(40);
plot(O,Fc26,'r');hold on;
plot(O,Fc25,'g');hold on
plot(O,Fc28,'b');hold on;
plot(O,Fc27,'k');hold off
xlabel('Degrees');
ylabel('Cam Tappet friction(N)');
title('Tappet Rotation');
legend('400 RPM at 40 C','400 RPM at 95 C','1000 RPM at 40 C','1000 RPM at 95 C');
print(f,'-djpeg', 'C:\Users\ars\Desktop\result\Fc2526.jpg');

f = figure(41);
```

```
plot(O,WL25,'r');hold on;
plot(O,WL26,'g');hold on
plot(O,WL27,'b');hold on;
plot(O,WL28,'k');hold off
xlabel('Degrees');
ylabel('Vertical loading(N)');
title('Tappet Rotation');
legend('400 RPM at 40 C','400 RPM at 95 C','1000 RPM at 40 C','1000 RPM at 95 C');
print(f,'-djpeg', 'C:\Users\ars\Desktop\result\WL2526.jpg');
ROtation and non raotation
w =400;
mewLimit =.12;
no=(9.72*10^-6)*1000;
Omega =200*.10471.*ones(1,360);

[hminrot,Omegarot,WLrot,Verot,hcenrot,Ttorquerot,Fcrot,v,a,Vs,R,avgOmega,totalpowerLosrot
] = atiqrotation(w,mewLimit,no,Omega,O,l,l1)
 w =400;
mewLimit =.12;
no=(9.72*10^-6)*1000;

[hmin,Omega,WL,Ve,hcen,Ttorque,Fc,v,a,Vs,R,avgOmega,totalpowerLos,powerLosYangrot,po
werLosroughrot] = atiq(w,mewLimit,no,Omega,O,l,l1)
f = figure(42);
plot(O,hminrot,'r');hold on;
plot(O,hmin,'k');hold off
xlabel('Degrees');
ylabel('Minimum film thickness (m)');
title('Minimum film thickness(m)');
legend('400 RPM at 95 C','400 RPM at 95 C');
print(f,'-djpeg', 'C:\Users\ars\Desktop\result\hminrotnonrot400.jpg');
```

```
f = figure(43);
plot(O,Fcrot,'r');hold on;
plot(O,Fc,'k');hold off
xlabel('Degrees');
ylabel('Friction');
title('Friction N');
legend('400 RPM at 95 C with rotation','400 RPM at without rotation 95 C');
print(f,'-djpeg', 'C:\Users\ars\Desktop\result\WLrotnonrot400.jpg');
w =1000;
mewLimit =.12;
no=(9.72*10^-6)*1000;
Omega =200*.10471.*ones(1,360);

[hminrot1,Omegarot1,WLrot1,Verot1,hcenrot1,Ttorquerot1,Fcrot1,v,a,Vs,R,avgOmega,totalpow
erLosrot1] = atiqrotation(w,mewLimit,no,Omega,O,l,l1)
 w =1000;
mewLimit =.12;
no=(9.72*10^-6)*1000;

[hminwrot,Omega,WL,Ve,hcen,Ttorque,Fcwrot,v,a,Vs,R,avgOmega,totalpowerLos2,powerLos
Yangrot,powerLosroughrot] = atiq(w,mewLimit,no,Omega,O,l,l1)
f = figure(44);
plot(O,hminrot1,'r');hold on;
plot(O,hminwrot,'k');hold off
xlabel('Degrees');
ylabel('Minimum film thickness (m)');
title('Minimum film thickness(m)');
legend('1000 RPM at 95 C with rotation','1000 RPM at 95 C');
print(f,'-djpeg', 'C:\Users\ars\Desktop\result\WLrotnonrot1000.jpg');
f = figure(45);
plot(O,Fcrot,'r');hold on;
```

```
plot(O,Fcwrot,'k');hold off
xlabel('Degrees');
ylabel('Friction N');
title('Friction N');
legend('1000 RPM at 95 C with rotation','1000 RPM at 95 C');
print(f,'-djpeg', 'C:\Users\ars\Desktop\result\WLrotnonrot1000.jpg');
```